



HAL
open science

Exploring the landscape and climatic conditions of Neanderthals and anatomically modern humans in the Middle East: the rodent assemblage from the late Pleistocene of Kaldar Cave (Khorramabad Valley, Iran)

Iván Rey-Rodríguez, Juan-Manuel López-García, Hugues-Alexandre Blain, Emmanuelle Stoetzel, Christiane Denys, Mónica Fernández-García, Laxmi Tumung, Andreu Ollé, Behrouz Bazgir

► To cite this version:

Iván Rey-Rodríguez, Juan-Manuel López-García, Hugues-Alexandre Blain, Emmanuelle Stoetzel, Christiane Denys, et al.. Exploring the landscape and climatic conditions of Neanderthals and anatomically modern humans in the Middle East: the rodent assemblage from the late Pleistocene of Kaldar Cave (Khorramabad Valley, Iran). *Quaternary Science Reviews*, 2020, 236, pp.106278 -. 10.1016/j.quascirev.2020.106278 . hal-03490475

HAL Id: hal-03490475

<https://hal.science/hal-03490475>

Submitted on 22 Aug 2022

HAL is a multi-disciplinary open access archive for the deposit and dissemination of scientific research documents, whether they are published or not. The documents may come from teaching and research institutions in France or abroad, or from public or private research centers.

L'archive ouverte pluridisciplinaire **HAL**, est destinée au dépôt et à la diffusion de documents scientifiques de niveau recherche, publiés ou non, émanant des établissements d'enseignement et de recherche français ou étrangers, des laboratoires publics ou privés.



Distributed under a Creative Commons Attribution - NonCommercial 4.0 International License

1 **EXPLORING THE LANDSCAPE AND CLIMATIC CONDITIONS OF**
2 **NEANDERTHALS AND ANATOMICALLY MODERN HUMANS IN THE**
3 **MIDDLE EAST: THE RODENT ASSEMBLAGE FROM THE LATE**
4 **PLEISTOCENE OF KALDAR CAVE (KHORRAMABAD VALLEY, IRAN)**

5
6 Iván Rey-Rodríguez ^{a,b,*}, Juan-Manuel López-García ^{c,d}, Hugues-Alexandre
7 Blain ^{c,d}, Emmanuelle Stoetzel ^a, Christiane Denys ^e, Mónica Fernández-García
8 ^{b,a}, Laxmi Tumung ^{c,d,a}, Andreu Ollé ^{c,d}, Behrouz Bazgir ^d

9
10 ^a HNHP UMR 7194, CNRS / Muséum national d'Histoire naturelle / UPVD / Sorbonne
11 Universités, Musée de l'Homme, Palais de Chaillot, 17 place du Trocadéro, 75016 Paris, France

12 ^b Sezione di Scienze Preistoriche e Antropologiche, Dipartimento di Studi Umanistici, Università
13 degli Studi di Ferrara, C.so Ercole I d'Este, 32 - 44121 Ferrara, Italy

14 ^c Institut Català de Paleoecologia Humana i Evolució Social (IPHES). Zona Educacional 4,
15 Campus Sescelades URV (Edifici W3) 43007 Tarragona, Spain

16 ^d Àrea de Prehistòria, Universitat Rovira i Virgili. Facultat de Lletres, Avinguda Catalunya 35,
17 43002 Tarragona, Spain

18 ^e ISYEB UMR 7205, CNRS / Muséum national d'Histoire naturelle / UPMC / EPHE / Sorbonne
19 Universités, Paris, France

20 * **corresponding author:** ivan.rey-rodriguez@edu.mnhn.fr / ivanreyrguez@gmail.com (Iván
21 Rey-Rodríguez)

22 **Abstract**

23 The Middle East, specially the Zagros region, lies in a strategic position as a
24 crossroads between Africa, Europe and eastern Asia. The landscape of this
25 region that prevailed around the Neanderthal and anatomically modern human
26 occupations is not well known. Only a few sites have been studied in detail in this
27 area, often providing only a faunal list. These reveal that Neanderthals and
28 anatomically modern humans lived in a landscape mainly composed of dry
29 steppes.

30 Here we extend the data obtained from Kaldar Cave through a systematic study
31 of the rodent assemblage. The site provided evidence of a Pleistocene
32 occupation attested by lithic tools associated with the Middle and Upper
33 Palaeolithic, but it was also occupied during the Holocene, as evidenced by

34 Neolithic artefacts. First excavations have revealed small vertebrates in Layer 4
35 (sub-layer 5 and 5II), belonging to the Upper Palaeolithic, and Layer 5 (sub-layers
36 7 and 7II), belonging to the Middle Palaeolithic.

37 The rodent assemblage of Kaldar Cave is mainly composed of six arvicoline, two
38 cricetine, one glirid, one dipodid, one gerbilline and two murine species.

39 This assemblage shows that during the Late Pleistocene the environment around
40 the site was mainly composed of open dry steppes, as indicated by the most
41 abundant taxa, *Microtus*, *Ellobius* and *Meriones*. However, murine species
42 indicate the presence of a vegetation cover. The palaeoclimatic conditions are
43 characterised by lower temperatures and also less precipitation than at present.

44 The results obtained with the rodent assemblages show that there is no major
45 palaeoenvironmental or palaeoclimatic change that would explain the cultural
46 shift between Layer 5 (Middle Palaeolithic) and Layer 4 (Upper Palaeolithic).

47 **Keywords:** *Rodentia*, *Middle East*, *taxonomy*, *palaeoecology*, *human*
48 *occupations*

49 **1. Introduction**

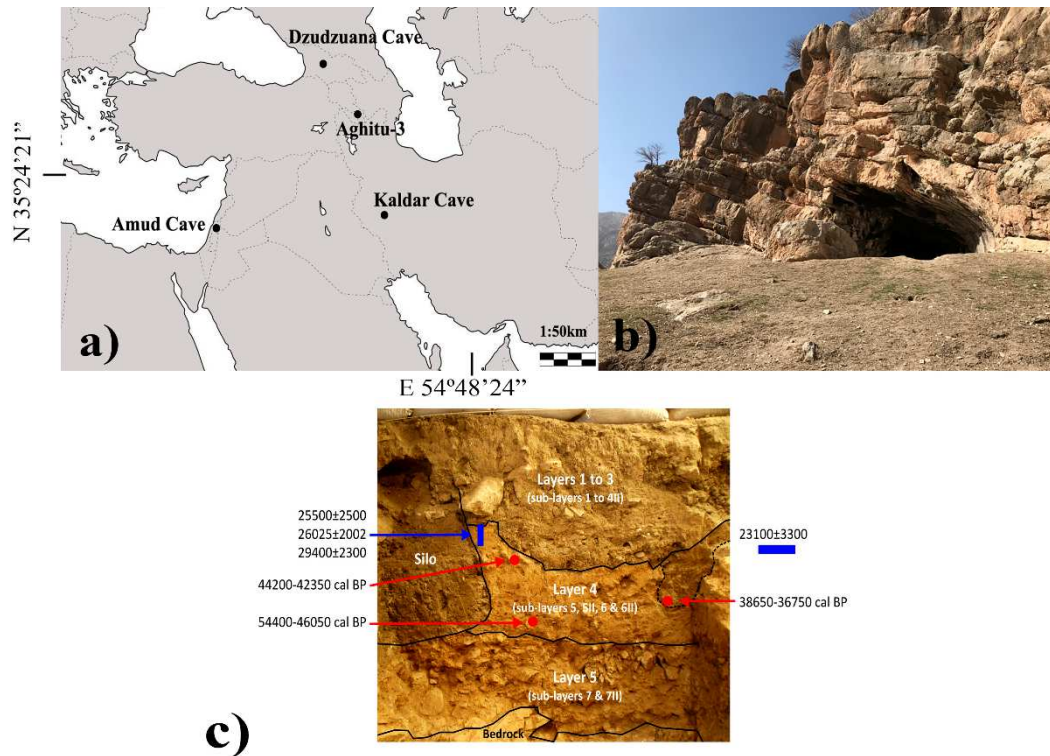
50 Small vertebrates are recognized to be good palaeoecological indicators due to
51 their rapid evolution, the limited geographic range of a species and unique niche
52 requirements, as well as their frequent preservation in archaeological and
53 palaeontological sites. They might be excellent indicators of palaeovegetation
54 type and provide a high-resolution proxy for palaeoenvironmental changes (e.g.
55 Belmaker and Hovers, 2011). Studies of small vertebrates from archaeological
56 sites in the Middle East are still scarce (Belmaker and Hovers, 2011; Belmaker
57 et al., 2016; Demirel et al., 2011; Fernández-Jalvo, 2016a; Kandel et al., 2017;
58 Maul et al., 2015a, 2015b; Smith et al., 2015; Weissbrod and Zaidner, 2014), and
59 they mainly propose preliminary lists of taxa. On the other hand, some studies of
60 extant owl pellet assemblages have been performed in the Middle East (Abi-said
61 et al., 2014; Darvish et al., 2000; Haddadian Shad et al., 2014; Kopij and Liven-
62 schulman, 2013; Obuch and Khaleghizadeh, 2012; Rey-Rodríguez et al., 2019;
63 Shehab et al., 2013), providing taxonomic and some taphonomic reference data
64 in Iran, Lebanon, Israel, Turkey and Syria.

65 The main palaeoecological and palaeoclimatic reconstructions based on faunal
66 assemblages relate to the unique niche requirements of a particular species.
67 Belmaker *et al.* (2011) pointed out that their interpretations, in contrast, are based
68 on analyses of community composition. Analyses of persistence *versus* change
69 over time should take into account species presence-absence, rank abundance
70 and proportional abundance (Belmaker and Hovers, 2011).

71 The Middle East is a prime location to study Neanderthal and anatomically
72 modern human (AMH) interactions during the Middle to Upper Palaeolithic
73 transition (Belmaker *et al.*, 2016). However, sites yielding evidence of both
74 Neanderthal and AMH occupations in the same sequence are rare, only five sites
75 were well excavated (Bazgir *et al.*, 2014; Bazgir *et al.*, 2017). In this framework,
76 Kaldar Cave is a key archaeological site for evaluating the influence of
77 environment on cultural changes in both human species because of its location
78 and the faunal and lithic remains. The main objective of this paper is to infer the
79 landscape composition and the climatic conditions in which Neanderthal and
80 AMH populations pursued their activities through the study of small mammals.
81 We identify and describe the rodent fossils recovered from Kaldar Cave in order
82 to establish the main criteria for further identifications in this region and provide a
83 preliminary basis for future systematic studies.

84 **2. Kaldar Cave**

85 Kaldar Cave is located in the northern part of the Khorramabad valley, Lorestan
86 Province, western Iran (48°17'35" E, 33°33'25" N) at 1290 m a.s.l. (Fig. 1a,b). The
87 cave was discovered in 2007, and the first archaeological intervention was
88 undertaken by an Iranian-Spanish team in 2011-2012, revealing the great
89 potential of the cave (Bazgir *et al.*, 2014). A second excavation was performed in
90 2014-2015. The trench exposed an approximately 2m-thick section of
91 sedimentary deposits, characterized by 5 main layers, themselves divided into
92 several sub-layers (Fig. 1c).



93

94 Figure 1: a) Locations of the Late Pleistocene sites with rodent studies in the
 95 Middle East, including Kaldar Cave. b) General view of the entrance to Kaldar
 96 Cave. c) Stratigraphy of the eastern section of Kaldar Cave, including the location
 97 and results of the dated samples, from A. Ollé and B. Bazgir (Bazgir et al., 2017).

98 Layer 5 (including sub-layers 7 and 7II) consists of an extremely cemented
 99 reddish-brown sediment with some small angular limestone blocks and Middle
 100 Palaeolithic artefacts with Levallois elements. So far, no chronometric data are
 101 available for this layer (Bazgir et al., 2017).

102 Layer 4 (including sub-layers 5, 5II, 6 and 6II) consists of a silty but compact dark-
 103 brown sediment with cultural remains attributed to the Upper and early Upper
 104 Palaeolithic. In the uppermost parts of this layer, two fireplaces made of clay were
 105 recovered and dated through thermoluminescence, yielding ages that ranged
 106 from 23,100 ± 3 300 to 29,400 ± 2 300 BP (Bazgir et al., 2017). The dates
 107 obtained show that these fireplaces were made or re-used from existing older
 108 sediment from the upper part of this layer in the later stages of the Upper
 109 Palaeolithic. AMS radiocarbon dates of 38,650–36,750 cal BP, 44,200–42,350
 110 cal BP, and 54,400–46,050 cal BP have been obtained from charcoal material
 111 located below this layer (Bazgir et al., 2017; Becerra-Valdivia et al., 2017).

112 Layers 1 to 3 (including sub-layers 4 and 4II) consist of ashy sediments of a
113 blackish-green colour containing both thick and thin angular limestone clasts.
114 These layers varied in thickness from 60 to 90 cm and contained many phases
115 dating to the Holocene: Islamic and historical eras, Iron Age, Bronze Age,
116 Chalcolithic and Neolithic. However, due to the presence in these layers of
117 bioturbation mainly by burrowing animals, the phases were recognized only by a
118 preliminary study of the potsherds, metal artefacts and some diagnostic lithic
119 artefacts from the lower layers.

120 This site provides evidence for the Middle to Upper Palaeolithic transition in the
121 Middle East (Bazgir et al., 2017). Moreover, Kaldar Cave has yielded the oldest
122 evidence of *Prunus* spp. in the area, through the study of thirty charcoal remains
123 (Allué et al., 2018), that helps us to reconstruct the environmental conditions,
124 evidencing a wooded vegetation.

125 **3. Material and methods**

126 The rodent fossil remains used in this study, 1112 molars, come from the
127 archaeological excavation campaigns carried out in Kaldar Cave in 2011-2012
128 and 2014-2015.

129 The samples comprise disarticulated bones and isolated teeth that were collected
130 in the field by water screening using superimposed 5 and 0.5 -mm mesh screens.

131 **3.1. Taxonomy**

132 In this article we only focus on rodents, because these are one of the most useful
133 tools for palaeoenvironmental and palaeoclimatic reconstructions of
134 archaeological sites, and the other material, as amphibians, squamates, birds,
135 shrews and bats, will be studied later. The taxonomic identification of the rodent
136 remains is based mainly on molar morphology and measurements of the lower
137 m1, the taxonomically most diagnostic tooth.

138 The remains were identified at a specific level whenever possible, thanks to
139 comparisons with reference collections from the Natural History Museum of
140 London (NHM) and comparative morphological and biometric data from the
141 literature, notably for *Microtus* (Coşkun, 2016; Kryštufek and Shenbrot, 2016;

142 Kryštufek and Vohralík, 2009; López-García, 2011; Rusin, 2017; Shenbrot,
143 Kryštufek et al. 2016; Tesakov, 2016), *Cricetulus* (Bogicevic et al., 2011;
144 Kryštufek et al., 2017; Sándor, 2018), *Mesocricetus* (Kryštufek and Vohralík,
145 2009), *Meriones* (Coşkun, 1999; Darvish, 2011; Dianat et al., 2017; Kryštufek and
146 Vohralík, 2009; Souttou and Denys, 2012; Stoetzel et al., 2017), *Allactaga*
147 (Karami et al., 2008; Shenbrot, 2009), *Myomimus* (Gerrie and Kennerley, 2017;
148 Karami et al., 2008; Kennerley and Kryštufek, 2019), *Apodemus* (Amori et al.,
149 2016; Bogicevic et al., 2011; Knitlová and Horáček, 2017; Kryštufek and Vohralík,
150 2009; López-García, 2008) and *Mus* (Darviche et al., 2006; Kryštufek and
151 Vohralík, 2009; Siahsarvie and Darvish, 2008).

152 Quantification of taxonomic frequencies was based on standard measures in
153 zooarchaeological analyses, including the number of identified specimens (NISP)
154 and minimum number of individuals (MNI) (Weissbrod and Zaidner, 2014). This
155 latter was estimated using the most abundant skeletal element present in the
156 assemblage (molars in our case).

157 **3.2. Taphonomy**

158 A preliminary study was performed on the Kaldar Cave micromammal remains.
159 This was based on the systematic descriptive method that examines the
160 modifications of prey bones induced by predation, focusing on the degree of
161 digestion observed in teeth during the identification (Andrews, 1990; Fernández-
162 Jalvo et al., 2016). This study showed a significant number of digested teeth
163 (Bazgir et al., 2017), indicating that predation activity was the origin of at least
164 part of the accumulation.

165 **3.3. Palaeoenvironmental and palaeoclimatic reconstructions**

166 *3.3.1. Habitat weighting method*

167 Palaeoecological interpretations derived from faunal data are based on analyses
168 of community composition (Belmaker and Hovers, 2011). The method used for
169 the palaeoenvironmental reconstruction is the *habitat weighting method*, also
170 named the *taxonomic habitat index* (Evans et al., 1981; Andrews, 2006; modified
171 by Blain et al., 2008; López-García et al., 2011), which is based on the current

172 distribution of each taxon in the habitat(s) where it can be found nowadays. We
 173 assume that the Kaldar Cave species had equivalent ecological requirements to
 174 their present-day relatives, because the Late Pleistocene species are the same
 175 as those today and no extinct fossil species are found in the assemblage. We
 176 adapt the method to our studied area, differentiating the following types of
 177 habitats: Forest (Fo), a large area covered with trees; Shrubland (Sh), vegetation
 178 dominated by shrubs; Grassland (Gr), an open area covered with grass; Desert
 179 (De), an area with little precipitation and no vegetation cover; Wetland (We), an
 180 area where water covers the soil; Steppe (St), a dry grassy plain; and Rocky (Ro),
 181 a rocky or stony substrate. Each species has a score of 1.00, which is divided
 182 between the habitats where the species can be found at present (Table 1), all the
 183 species ranges were taken from the IUCN Red List of Threatened Species
 184 (<https://www.iucnredlist.org/resources/spatial-data-download>).

Species	Fo	Sh	Gr	De	We	St	Ro
<i>Ellobius lutescens</i>			0.33	0.33		0.33	
<i>Ellobius fuscocapillus</i>						1	
<i>Microtus irani</i>			1				
<i>Microtus guentheri</i>			1				
<i>Microtus socialis</i>		0.5				0.5	
<i>Chionomys nivalis</i>							1
<i>Cricetulus migratorius</i>			0.33	0.33		0.33	
<i>Mesocricetus brandti</i>						1	
<i>Meriones persicus</i>		0.33	0.33				0.33
<i>Allactaga</i> sp.				0.5		0.5	
<i>Apodemus</i> sp.	1						
<i>Mus musculus</i>		0.33	0.33		0.33		
<i>Myomimus</i> sp.				1			

185

186 Table 1: scores attributed to each rodent species found at Kaldar Cave according
 187 to its ecological requirements, used for the *habitat weighting method*: Forest (Fo),
 188 Shrubland (Sh), Grassland (Gr), Desert (De), Wetland (We), Steppe (St) and
 189 Rocky (Ro).

190 3.3.2. Bioclimatic Model

191 In order to reconstruct the climate at Kaldar Cave, we applied the *bioclimatic*
 192 *model (BM)*, which was developed by Hernández-Fernández (2001) on the basis
 193 of the faunal spectrum, assuming that small- and large-mammal species can be

194 ascribed to ten different climates (Hernández-Fernández, 2001; Hernández-
 195 Fernández and Peláez-Campomanes, 2003; Hernández-Fernández et al., 2007).
 196 It was first necessary to calculate the climatic restriction index ($CRI_i = 1/n$, where i
 197 is the climatic zone where the species appear and n is the number of zones where
 198 the species is present) and the bioclimatic component ($BC_i = (\sum CRI_i) 100/S$,
 199 where i is the climatic zone and S is the number of species). To BC a
 200 mathematical model is applied as a regression that allows us to calculate climatic
 201 parameters (see Appendix 1).

202 The different climatic groups defined by Hernández-Fernández (2001) and
 203 Hernández-Fernández et al. (2007) are: I *equatorial*; II *tropical with summer rains*;
 204 II/III *transition tropical semiarid*; III *sub-tropical arid*; IV, *subtropical* with winter
 205 rains and summer droughts; V, *warm temperate* with not very severe winters but
 206 high humidity; VI, *typical temperate* with winters that are cold but not very long,
 207 but summers that are cool; VII, *arid-temperate* with large temperature contrasts
 208 between winter and summer; VIII, *cold-temperate* with cool summers and long
 209 cold winters (boreal) and IX, *artic* (Table 2).

Species	I	II	II/III	III	IV	V	VI	VII	VIII	IX
<i>Ellobius lutescens</i>								1		
<i>Ellobius fuscocapillus</i>				0.33	0.33			0.33		
<i>Microtus irani</i>					1					
<i>Microtus socialis</i>					0.5			0.5		
<i>Chionomys nivalis</i>					0.25		0.25		0.25	0.25
<i>Cricetulus migratorius</i>					0.33		0.33	0.33		
<i>Mesocricetus brandti</i>					1					
<i>Meriones persicus</i>				0.5	0.5					
<i>Allactaga</i> sp.				0.5				0.5		
<i>Apodemus</i> sp.							1			
<i>Mus musculus</i>	0.11	0.11	0.11	0.11	0.11	0.11	0.11	0.11	0.11	

210

211 Table 2: scores attributed to each rodent species found at Kaldar Cave for the
 212 bioclimatic model (in accordance with Hernández-Fernández, 2001; Hernández-
 213 Fernández et al., 2007). See text for the significance of the Roman numerals
 214 corresponding to the climatic groups.

215 By means of the *BM* we were able to estimate the mean annual temperature
 216 (MAT), the mean temperature of the coldest month (MTC), the mean temperature
 217 of the warmest month (MTW) and the mean annual precipitation (MAP). This

218 method also allowed us to assess whether there were changes in the temperature
219 and precipitation regimes during the Middle to Upper Palaeolithic transition at
220 Kaldar Cave.

221 **4. Results and discussion**

222 **4.1. Taxonomic identifications**

223 In total 264 minimum number of individuals (MNI) were identified (Table 3 and
224 Fig. 2). Some differences were found with respect to the preliminary list previously
225 published by Bazgir et al. (2017). We notably found some new specimens and
226 reconsidered the identifications for *Ellobius talpinus*, *Calomyscus* sp. and
227 *Dryomys* cf. *nitedula*.



228

229 Figure 2: Some rodent species identified at Kaldar Cave in comparison with
 230 equivalent (analogue) modern specimens from the NHM of London. **1) *Microtus***
 231 ***irani***: 1.1-Kaldar Cave, 2014, Layer 5 (sub-layer 7II), E7, 150-156, right lower
 232 m1, number 447. 1.2-modern, NHM205207, Iran (Shiraz), right lower m1; **2)**
 233 ***Microtus guentheri***: 2.1-Kaldar Cave, 2014, Layers 1-3 (sub-layer 4II), F6, 97-
 234 107, left lower m1, number 17; **3) *Microtus socialis***: 3.1-Kaldar Cave, 2014,
 235 Layer 4 (sub-layer 5II), F7, 115-118, right lower m1, number 106. 3.2-modern,
 236 NHM631799, Turkey (Amasya); **4) *Chionomys nivalis***: 4.1-Kaldar Cave, 2014,
 237 Layer 4 (sub-layer 5), E6, 94-104, left lower m1, number 542. 4.2-modern,

238 NHM71820, Syria, left lower m1; **5) *Ellobius fuscocapillus***: 5.1-Kaldar Cave,
239 2014, Layer 4 (sub-layer 5II), E6, 125-130, right lower m1, number 157. 5.2-
240 modern, NHM86101513, Afghanistan, right lower m1; **6) *Ellobius lutescens***:
241 6.1-Kaldar Cave, 2014, Layer 5 (sub-layer 7II), F6, 130-140, right lower m1,
242 number 319. 6.2-NMH916416, Turkey, right lower m1; **7) *Cricetulus***
243 ***migratorius***: 7.1- Kaldar Cave, 2014, Layer 4 (sub-layer 5II), E6, 135-140, left
244 lower m1, number 259. 7.2-modern, NHM773029, Iran, right lower m1; **8)**
245 ***Mesocricetus brandti***: 8.1-Kaldar Cave, 2014, Layer 5 (sub-layer 7II), F6, 135-
246 145, left upper M1, number 549. 8.2- modern, NHM193461226, Caucasus, left
247 upper M1; **9) *Meriones cf. persicus***: 9.1-Kaldar Cave, 2014, Layer 5 (sub-layer
248 7II), F6, 156-166, left lower m1, number 551. 9.2-modern, NHM510434, Iran, left
249 lower m1; **10) *Allactaga sp.***: 10.1-Kaldar Cave, 2014, Layer 5 (sub-layer 7II), E7,
250 141-147, right lower m3, number 203; **11) *Myomimus sp.***: 11.1- Kaldar Cave,
251 2014, Layer 5 (sub-layer 7II), E7, 141-147, left lower m1 and m2. 11.2-modern,
252 ***Myomimus personatus***, NHM67623, Turkey, left lower mandible; **12)**
253 ***Apodemus sp.***: 12.1-Kaldar Cave, 2014, Layer 4 (sub-layer 5), E6, 94-104, right
254 m1 and m2, number 547; **13) *Mus cf. musculus***: 13.1-Kaldar Cave, 2014, Layer
255 5 (sub-layer 7II), 166-174, left lower m1, number 495. Scale 1 mm

Taxon	Layer 5			Layer 4			Layers 1-3		
	NISP	MNI	NISP%	NISP	MNI	NISP%	NISP	MNI	NISP%
Indet.	3	-	-	11	-	-	-	-	-
<i>Microtus</i> spp.	292	51	52.33	258	31	48.31	4	3	20
<i>Microtus irani</i>	14	9	2.51	0	0	0.00	1	1	5
<i>Microtus guentheri</i>	0	0	0.00	16	9	3.00	1	1	5
<i>Microtus socialis</i>	35	20	6.27	36	20	6.74	3	3	15
<i>Chionomys nivalis</i>	6	3	1.08	17	12	3.18	2	1	10
<i>Ellobius</i> spp.	80	7	14.34	91	8	17.04	2	2	10
<i>Ellobius fuscocapillus</i>	5	4	0.90	5	3	0.94	1	1	5
<i>Ellobius lutescens</i>	10	6	1.79	10	7	1.87	-	-	-
<i>Cricetulus migratorius</i>	5	3	0.90	14	3	2.62	1	1	5
<i>Mesocricetus brandti</i>	7	4	1.25	3	1	0.56	0	0	0
<i>Meriones cf. persicus</i>	88	18	15.77	65	17	12.17	3	2	15
<i>Allactaga sp.</i>	1	1	0.18	1	1	0.19	0	0	0
<i>Myomimus sp.</i>	5	3	0.90	0	0	0.00	0	0	0
<i>Apodemus sp.</i>	5	2	0.90	6	3	1.12	2	1	10
<i>Mus cf. musculus</i>	2	1	0.36	1	1	0.19	0	0	0
Total	558	132	100.00	534	116	100.00	20	16	100.00

256 Table 3: Representation of the Kaldar Cave rodent species in terms of number of
257 identified specimens (NISP), minimum number of individuals (MNI) and
258 percentage of the NISP (%).

259 **Order Rodentia Bowdich, 1821**

260 **Rodentia indet.**

261 There are 14 teeth (11 in Layer 4 and 3 in Layer 5) that have not been identified
262 to the family or genus level because they were broken.

263 **Family Cricetidae Fisher, 1817**

264 **Subfamily Arvicolinae Gray, 1821**

265 **Genus *Microtus* Schrank, 1798**

266 ***Microtus* spp.**

267 **Material:** 554 isolated teeth. **Layer 1-3:** four isolated teeth; three left lower m1
268 and one right lower m1. **Layer 4:** 258 isolated teeth; 81 m2; 101 m3, 13 right
269 upper M1, 31 right lower m1; four left upper M1 and 28 left lower m1. **Layer 5:**
270 292 isolated teeth; 119 m2; 53 m3; nine left upper M1, 51 left lower m1; 10 right
271 upper M1; 50 right lower m1.

272 ***Microtus socialis* Pallas, 1773**

273 **Material:** 74 isolated teeth. **Layer 1-3:** three isolated teeth, three right lower m1.
274 **Layer 4:** 36 isolated teeth; 20 right lower m1 and 16 left lower m1. **Layer 5:** 35
275 isolated teeth; 20 right lower m1 and 15 left lower m1.

276 ***Microtus irani* Thomas, 1921**

277 **Material:** 15 isolated teeth. **Layer 1-3:** one isolated tooth, one right lower m1.
278 **Layer 5:** 14 isolated teeth; nine right lower m1 and five left lower m1.

279 ***Microtus quentheri* Danford & Alston, 1880**

280 **Material:** 17 isolated teeth. **Layer 1-3:** one isolated tooth, one left lower m1.
281 **Layer 4:** 16 isolated teeth; nine right lower m1 and seven left lower m1.

282 **Description and discussion:** all the molars are hypsodont and arhizodont with
 283 crown cementum in the re-entrant angles. The enamel differentiation is *Microtus*-
 284 like. Six extant species of *Microtus* have been identified in Iran: *Microtus arvalis*,
 285 *Microtus irani*, *Microtus kermanensis*, *Microtus socialis*, *Microtus transcaspicus*
 286 and *Microtus guentheri* (Aşan Baydemir and Duman, 2009; Golenishchev et al.,
 287 2019; Firouz, 2005).

288 *Microtus* m1 are characterized by four buccal and five lingual re-entrant angles
 289 (Kryštufek and Vohralík, 2009; Tsytsulina et al., 2017) with a posterior lobe (PL),
 290 seven triangles (T) and an anterior cap (AC). We identified the Kaldar specimens
 291 on the basis of their measurements (Table 4), the arrangement and morphology
 292 of the triangles, and the AC (which may or may not be connected with the other
 293 elements).

Species	NS	L (Length)		La (Width T4)		Li (Width T5)		Total Width	
		Mean	Min-Max	Mean	Min-Max	Mean	Min-max	Mean	Max-Min
<i>Microtus irani</i>	4	3.06	2.98-3.23	0.42	0.40-0.44	0.64	0.62-0.67	1.06	1.03-1.08
<i>Microtus socialis</i>	69	2.78	2.29-3.34	0.42	0.32-0.51	0.6	0.44-0.73	1.02	0.78-1.19
<i>Microtus arvalis</i>	25	2.72	2.45-2.96	0.39	0.32-0.46	0.6	0.50-0.70	1	0.83-1.13
<i>Microtus guentheri</i>	70	2.58	2.2-3						
Kaldar Cave									
<i>Microtus guentheri</i>	17	2.52	2.18-3.01	0.35	0.27-0.43	0.54	0.40-0.68	0.90	0.70-1.10
<i>Microtus irani</i>	15	2.89	2.52-3.39	0.41	0.37-0.50	0.62	0.54-0.70	1.05	0.92-1.18
<i>Microtus socialis</i>	74	2.54	2.06-3.01	0.37	0.28-0.48	0.55	0.40-0.70	0.92	0.70-1.16

294 Table 4: Measurements of *Microtus* specimens (in mm): NS, number of
 295 specimens; L, length; La, T4 width; Li, T5 width.

296 In our sample we identified *Microtus* spp., *Microtus socialis*, *Microtus guentheri*
 297 and *Microtus irani*.

298 In *Microtus socialis*, the triangles from T1-T5 are closed, but T6-T7 are parallel
 299 and broadly confluent with the AC. *Microtus guentheri* is distinguishable from
 300 *Microtus socialis* by the rounded shape of the AC, which is of an arhombomorph
 301 type (Aşan Baydemir and Duman, 2009), and also by T6-T7, which are separated

302 from the AC. In accordance with the measurements given in Aşan Baydemir et
303 al. (2009), the size of *Microtus guentheri* and *Microtus socialis* is similar. In
304 *Microtus irani*, triangles T1-T5 are closed, but T6-T7 are open and not parallel
305 with one another; moreover, *Microtus irani* is clearly larger than the other species
306 considered in our reference collection and also in our sample. Finally, we include
307 in *Microtus* spp. all the elements that we cannot attribute to one species or
308 another, in particular because of their bad state of preservation (due to digestion,
309 breakage).

310 **Habitat and distribution:** *Microtus irani* occupies grasslands in Iran, Turkey and
311 the Caucasus (Kryštufek and Kefelioğlu, 2001).

312 *Microtus socialis* is found in Russia, Ukraine, the Caucasus, Transcaucasia,
313 Turkestan, Iran and Afghanistan (Tsytulina et al., 2017), although the range is
314 fragmented. It is a highly colonial species, found in steppe habitats and also in
315 agricultural lands, but extending also to bushy scrubs and uncultivated mountain
316 valleys, as well as to open oak forests on dry hillsides (Tsytulina et al., 2017).

317 *Microtus guentheri* occurs from the southeastern Balkans and Turkey through
318 Syria, Lebanon and Israel, with an isolated range segment in northern Libya, Iran
319 and some parts of Europe (Aşan Baydemir and Duman, 2009). This species is
320 present in dry grasslands with sparse vegetation (Amr, 2015).

321 **Genus *Chionomys* Miller, 1908**

322 ***Chionomys nivalis* Martins, 1842**

323 **Material:** 25 isolated teeth. **Layer 1-3:** two isolated teeth; one left lower m1 and
324 one right lower m1. **Layer 4:** 17 isolated teeth; 12 right lower m1; five left lower
325 m1. **Layer 5:** six isolated teeth; three left lower m1; three right lower m1.

326 **Description and discussion:** in our specimens it can be observed that the first
327 lower molars display five triangles and that the morphology of the anteroconid
328 complex (AC) is characteristic of the *nivalis* morphotype, where triangles T6 and
329 T7 are absent and the anterior cap is of an arrowhead or oval shape, inclined
330 towards the labial part. The enamel is of the *Microtus* type with cement (Kryštufek,
331 2017; Kryštufek and Vohralík, 2009; López-García, 2011). These specimens

332 differ from *Microtus* in that they only have five triangles, and the morphology of
333 the AC is the other main characteristic of this species that helps us to differentiate
334 it from *Microtus*.

335 **Habitat and distribution:** *Chionomys nivalis* has a global distribution extending
336 from southwestern Europe through southeastern Europe to the Caucasus,
337 Turkey, Israel, Lebanon, Syria and Iran. In Iran it is distributed in the north and
338 also in the west (Shenbrot and Krasnov, 2005; Krystufek, 2017). This is the only
339 *Chionomys* species occurring today in Iran, but two other species (*C. gud*, *C.*
340 *roberti*) are represented a little further north (northeastern Turkey, southern
341 Georgia).

342 Regarding its habitat, it is present in open rocky areas, typically above the tree
343 line and with scarce vegetation cover (Amori, 1999).

344 **Genus *Ellobius* Fischer, 1814**

345 ***Ellobius* spp.**

346 **Material:** 173 isolated teeth. **Layer 1-3:** two isolated teeth; two left lower m1.
347 **Layer 4:** 91 isolated teeth; seven indet.; eight right lower m1; five left lower m1;
348 11 upper M1; 43 m2; 17 m3. **Layer 5:** 80 isolated teeth; seven left lower m1; three
349 upper M1; 45 m2; 25 m3.

350 ***Ellobius fuscocapillus* Blyth, 1843**

351 **Material:** 11 isolated teeth. **Layer 1-3:** one isolated tooth; one right lower m1.
352 **Layer 4:** five isolated teeth; two right lower m1; three left lower m1. **Layer 5:** five
353 isolated teeth; four left lower m1 and one right lower m1.

354 ***Ellobius lutescens* Thomas, 1897**

355 **Material:** 20 isolated teeth. **Layer 4:** 10 isolated teeth; seven right lower m1 and
356 three left lower m1. **Layer 5:** 10 isolated teeth; four left lower m1 and six right
357 lower m1.

358 **Description and discussion:** 204 isolated teeth show the typical traits of the
359 genus *Ellobius* (Miller, 1896; Hinton, 1962, Kretzoi, 1969; Coşkun, 2016;
360 Kryštufek & Shenbrot, 2016; Kryštufek and Vohralík, 2009; Rusin, 2017;

361 Shenbrot et al., 2016; Tesakov, 2016). *Ellobius* molars are notably characterized
 362 by the presence of roots that are well visible in adults and old individuals, but not
 363 always apparent in young specimens (Coşkun, 2016). Moreover, *Ellobius* molars
 364 lack cement in the re-entrant angles. The *Ellobius* m1 is composed of the anterior
 365 cap (AC), five triangles (T) with three buccal and four lingual salient angles, and
 366 one posterior lobe (PL). Both M3 and m3 are reduced and smaller than the other
 367 molars, with three triangles on the labial side and two triangles on the lingual side.
 368 M1 has three inner and outer folds, and M2 and M3 have two inner and two outer
 369 re-entrant folds. The first and second upper molars have three triangles on the
 370 lingual and labial sides. However, the re-entrant angle between the first and the
 371 second triangles on the lingual side is more superficial (Gharkheloo and Kıvanç,
 372 2003).

373 In Iran, the genus *Ellobius* is currently represented by three species: *Ellobius*
 374 *fuscocapillus*, *Ellobius lutescens* and *Ellobius talpinus* (Firouz, 2005; Kryštufek &
 375 Shenbrot, 2016; Kryštufek and Vohralík, 2009; Moradi Gharkheloo, 2003; Rusin,
 376 2017; Shenbrot et al., 2016). The m1 is quite similar among these species, but
 377 there are some differences that can help us to differentiate them.

378 The AC is broad in *Ellobius lutescens*, narrow in *Ellobius talpinus* and elongated
 379 in *Ellobius fuscocapillus* (Maul et al., 2015b). The distance between T4 and T5
 380 (W) and the total length (L) differ among the species (Table 5). We have observed
 381 in modern specimens from the Natural History Museum of London that *Ellobius*
 382 *fuscocapillus* is the largest and *Ellobius talpinus* the smallest.

		<i>Ellobius fuscocapillus</i>			<i>Ellobius lutescens</i>		<i>Ellobius talpinus</i>		
		Layer 5, NISP=5	Layer 4, NISP=5	Layer 1-3, NISP=1	NHM, NISP=12	Layer 5, NISP=9	Layer 4, NISP=10	NHM, NISP=14	NHM, NISP=14
L	Min-	3.29-	3.73-3.74	-	3.06-	3.08-3.32	3.05-3.4	3.07-3.3	2.86-3.35
	Max	3.84			4.05				
	Mean	3.45			3.53				
W	Min-	1.32-	1.40-1.54	-	1.3-1.59	1.20-1.45	1.13-1.48	1.11-1.52	1.09-1.72
	Max	1.51			1.41				
	Mean	1.45			1.41				

383

384 Table 5: Measurements of *Ellobius* specimens (in mm): L, total length; W, width.
385 NHM: Natural History Museum of London. NISP: number of identified specimens.

386 In our sample we identify as *Ellobius* spp. those m1s that are too broken or
387 digested to distinguish, as well as all the m2, m3, M1, M2 and M3 because of the
388 lack of discriminant characters. The identification of *Ellobius lutescens* and
389 *Ellobius fuscocapillus* in the Kaldar material is based on the morphology of the
390 AC and the measurements (L and W). We do not identify *Ellobius talpinus* in our
391 sample, as no specimen displays morphological features characteristic of this
392 species, such as the narrow AC, and because the measured specimens are
393 larger than *E. talpinus*.

394 **Habitat and distribution:** *Ellobius* species frequent steppes, grasslands and
395 semi-deserts in eastern Europe and central Asia; these fossorial species are
396 specialised in subterranean life (Coşkun, 2016; Kryštufek and Vohralík, 2009).
397 *Ellobius lutescens* is a Palaearctic species distributed across Iran, Iraq,
398 Azerbaijan, Armenia, Transcaucasia and East Anatolia (Thomas, 1905; Ellerman
399 and Morrison-Scott, 1951; Darlington, 1957; Osborn, 1962; Walker, 1964; Lay,
400 1967; Hassinger, 1973; Roberts, 1977; Corbet, 1978; Corbet and Hill, 1991;
401 Wilson and Reeder, 2005; Coşkun, 1997, 2016; Nowak, 1999; Kryštufek &
402 Shenbrot, 2016). In Iran, this species is found in mountain grasslands, sandy
403 semi-deserts and steppe areas (Kryštufek & Shenbrot, 2016; Tesakov, 2016).
404 *Ellobius fuscocapillus* shows a wide range across eastern Iran, Turkmenistan,
405 Afghanistan and Pakistan. In Iran it is found in open steppes with loose soil
406 (Shenbrot, Kryštufek & Molur, 2016).

407 **Subfamily Cricetinae Fischer, 1817**

408 **Genus *Cricetulus* Milne-Edwards, 1867**

409 ***Cricetulus migratorius* Pallas, 1773**

410 **Material:** 19 isolated teeth. **Layer 1-3:** one isolated tooth; one right lower m3.
411 **Layer 4:** 13 isolated teeth; three left lower m1, two left upper M2; three right lower
412 m1, three right upper M1 and two right upper M2. **Layer 5:** five isolated teeth;
413 three left lower m1 and two right lower m1.

414 **Description and discussion:** the first molars (m1 and M1) are brachyodont and
415 cuspidate, with two longitudinal series of cusps. Each series of cusps consists of
416 three pairs. The m1 and M1 are the largest and the m3/M3 the smallest. The
417 lower m3 only has two pairs of cusps (Kryštufek and Vohralík, 2009). We identify
418 *Cricetulus migratorius* in all the layers of Kaldar Cave in accordance with the
419 measurements and identification keys for molars based on the morphology and
420 arrangement of the tubercles and cusps provided by Kryštufek and Vohralík
421 (2009). We also draw comparisons with the reference collection from Iran,
422 Afghanistan and Azerbaijan housed in the Natural History Museum of London.
423 The grey hamster, or migratory hamster, is the smallest hamster species
424 (Bogicevic et al., 2011; Sándor, 2018).

425 **Habitat and distribution:** *Cricetulus migratorius* extends from eastern Europe
426 through Russia and central Asia to Mongolia and western China (Kryštufek et al.,
427 2017; Kryštufek and Vohralík, 2009). In Iran, this species is found all over the
428 country. The habitats of this species are mostly dry grasslands, steppes and
429 semi-deserts. Arid areas with relatively sparse vegetation are preferred
430 (Kryštufek et al., 2017; Maul et al., 2015a).

431 **Genus *Mesocricetus* Nehring, 1898**

432 ***Mesocricetus brandti* Nehring, 1898**

433 **Material:** 10 isolated teeth. **Layer 4:** three isolated teeth; one left upper M1, one
434 right lower m1 and one right upper M1. **Layer 5:** seven isolated teeth; four left
435 upper M1, one right upper M2 and two right upper M1.

436 **Description and discussion:** the specimens from Kaldar Cave are attributed to
437 *Mesocricetus brandti* on the basis of the size and morphology of the teeth. The
438 molars present a similar morphological pattern to *Cricetulus migratorius*, but are
439 significantly larger in size. The first molars have six tubercles, the second and
440 third molars only four. The largest molars are m1 and M1, whereas m2/M2 and
441 m3/M3 are reduced (Kryštufek and Vohralík, 2009). In Iran we also find
442 *Mesocricetus raddei*, which presents a similar morphology of the teeth to
443 *Mesocricetus brandti*, but compared with the NHM reference collection of the
444 latter, *Mesocricetus raddei* is bigger

445 **Habitat and distribution:** *Mesocricetus brandti* has the largest distributional
446 area of the species belonging to the genus *Mesocricetus*, ranging from Anatolia,
447 Transcaucasia (Armenia, Georgia and Azerbaijan) and southeast Dagestan to
448 northwest Iran (Qazvin in the east, Lorestan in the south; Lay, 1967). This species
449 is found at altitudes from sea level up to 2,600 m. However, the primary range is
450 from 1,000-2,200 m. *Mesocricetus brandti* is found in arid and semi-arid steppe
451 habitats in lowlands and in mountainous areas (Kryštufek et al., 2015; Kryštufek
452 and Vohralík, 2009; Neumann et al., 2017)

453 **Family Muridae Illiger, 1811**

454 **Subfamily Gerbillinae Gray, 1825**

455 **Genus *Meriones*, Illiger 1811**

456 ***Meriones* cf. *persicus* Blanford, 1875**

457 **Material:** 157 isolated teeth. **Layer 1-3:** three isolated teeth; two left upper M1
458 and one right lower m1. **Layer 4:** 65 isolated teeth; 21 m2; four m3; 17 left lower
459 m1; eight right upper M1, five left upper M1; 10 right lower m1. **Layer 5:** 88
460 isolated teeth; eight m3; 21 m2; 18 left lower m1, 10 left upper M1, 16 right upper
461 M1 and 15 right lower m1.

462 **Description and discussion:** the genus *Meriones* is one of the most diverse
463 among the tribe Gerbillini in the Palaeartic region, particularly in arid regions of
464 Asia (Darvish et al., 2011; Denys, 2017). The *Meriones* species reported in Iran
465 are: *Meriones crassus*, *Meriones hurrianae*, *Meriones lybicus*, *Meriones*
466 *meridianus*, *Meriones persicus*, *Meriones tristrami*, *Meriones vinogradovi* and
467 *Meriones zarudnyi* (Darvish, 2011; Dianat et al., 2017; Kryštufek and Vohralík,
468 2009; Souttou and Denys, 2012).

469 The material from Kaldar Cave attributed to the genus *Meriones* displays the
470 typical morphology of this group, including semi-hypsodont molars with prismatic
471 enamel triangles linked by a longitudinal crest and with no trace of cusps. In our
472 sample, we identify first upper molars (M1) with three roots, which is characteristic
473 of *Meriones persicus* and *Meriones tristrami*. Unfortunately, the dental
474 morphology of *Meriones persicus* and *Meriones tristrami* is very similar; there are

475 three roots in m1, the second molars have two transverse plates and two roots,
476 whereas the third molars are simple and rounded with a single root (Coşkun,
477 2016; Kryštufek and Vohralík, 2009).

478 Given its current distribution and the morphological traits observed in the
479 reference collection from Iran, Azerbaijan and Pakistan housed in the Natural
480 History Museum of London, we provisionally attribute our specimens to *Meriones*
481 cf. *persicus*, especially in the light of the number of roots and the morphology of
482 M1 and m1, pending a revision of the Middle Eastern species of the genus.

483 **Habitat and distribution:** the genus *Meriones* is distributed across North Africa,
484 Central Asia, Transcaucasia, Turkey and Pakistan (Darvish et al., 2014; Stoetzel
485 et al., 2017). It lives mostly in dry steppes of short or tall grass, on open hillside,
486 among rocky outcrops in desolate steppes, or in open dry meadows. The
487 distribution of *Meriones persicus* ranges from the Caucasus (including the
488 southeastern foothills of the Lesser Caucasus and the Talysh Plateau in
489 Azerbaijan) in the west, through northeastern Iraq and Iran to Turkmenistan,
490 Afghanistan (Habibi, 2004) and Pakistan, where it is widely distributed. It
491 generally occurs in arid, rocky or mountainous regions (Kryštufek and Vohralík,
492 2009; Molur & Sozen, 2016).

493 **Family Dipodidae Fischer, 1817**

494 **Genus *Allactaga* Cuvier, 1837**

495 ***Allactaga* sp.**

496 **Material:** two isolated teeth. **Layer 4:** one indet. **Layer 5:** one right lower m3.

497 **Description and discussion:** this rodent group is poorly known in the Middle
498 East (Shenbrot, 2009) and sometimes there is a size overlap between the
499 species. In our sample, we only found two items attributed to *Allactaga* sp. on the
500 basis of the complete lower m3, which presents a morphology with two inner folds
501 and one outer fold; the other tooth is broken, which prevents any precise
502 identification.

503 **Habitat and distribution:** in Iran four species are currently present: *Allactaga*
504 *elater*, *Allactaga euphratica*, *Allactaga firouzi* and *Allactaga hotsoni* (Karami et
505 al., 2008). The different species are morphologically very close and remain poorly
506 studied. They are mainly found in steppe vegetation and semi-desert areas
507 (Shenbrot, 2009).

508 **Family Gliridae Thomas, 1897**

509 **Genus *Myomimus* Ognev, 1924**

510 ***Myomimus* sp.**

511 **Material:** five isolated teeth, **Layer 5:** five isolated teeth, one right lower m1, three
512 right lower m2 and one left lower m2.

513 **Description and discussion:** the genus *Myomimus* is present in Iran with two
514 species, *Myomimus personatus* and *Myomimus setzeri* (Firouz, 2005; Gerrie &
515 Kennerley, 2017; Karami et al., 2008; Kennerley & Kryštufek, 2019). Regarding
516 the remains found at Kaldar, the m1 is of a trapezium-like shape, and its anterior
517 part tends to be narrower than the posterior part. The m1 has three roots, two in
518 the anterior part and one in the posterior part. The m2 is subrectangular, and its
519 occlusal pattern is simpler than in the m1. There are three roots in total, two in
520 the anterior part and one in the posterior part (Kaya and Kaymakçı, 2018;
521 Kryštufek and Vohralík, 2009). The two species are similar to one another and
522 poorly studied. Consequently, we were unable to identify the Kaldar material
523 precisely. Moreover, the reference collection of the Natural History Museum of
524 London only houses *Myomimus personatus* specimens, which could therefore
525 not be compared with *Myomimus setzeri*.

526 **Habitat and distribution:** these species are not well known as regards their
527 distribution. They are mainly found in desert areas (Gerrie & Kennerley, 2017;
528 Kennerley & Kryštufek, 2019).

529 **Family Muridae Illiger , 1811**

530 **Genus *Apodemus* Kaup, 1829**

531 **Apodemus sp.**

532 **Material:** 13 isolated teeth. **Layer 1-3:** two isolated teeth; one left lower m1 and
533 one left lower m2; **Layer 4:** six isolated teeth; three left lower m1, two right lower
534 m1 and one left upper M1. **Layer 5:** five isolated teeth; two left lower m1, one
535 right lower m1, one right upper M1 and one m2.

536 **Description and discussion:** the first lower molar (m1) can be seen to present
537 a low occlusal surface with six main cusps. The anterolabial and posterolabial
538 cusps of m1 converge in an X-shape. The posterior cusp of m1 is low, rounded
539 and well developed, with two or three secondary cusps in the labial part, and a
540 mesial tubercle. We attribute the remains found in Kaldar Cave to *Apodemus* sp.
541 because they present the traits characteristic of the genus *Apodemus* (Amori et
542 al., 2016; Bogicevic et al., 2011; Knitlová and Horáček, 2017; Kryštufek and
543 Vohralík, 2009; López-García, 2008).

544 **Habitat and distribution:** five *Apodemus* species are currently recognized in
545 Iran: *A. hyrcanicus*, *A. flavicollis*, *A. witherbyi*, *A. avicennicus* and *A. uralensis*, all
546 belonging to the *Sylvaemus* sub-genus (Jangjoo et al., 2011). *Apodemus* has a
547 large distribution range extending from Great Britain across much of continental
548 Europe to the Urals. It also extends east through Turkey to western Armenia, the
549 Zagros Mountains of Iran and south to Syria, Lebanon and Israel. It inhabits a
550 variety of woodland habitats (Amori et al., 2016).

551 **Genus *Mus* Linnaeus, 1758**

552 ***Mus cf. musculus* Linnaeus, 1758**

553 **Material:** three isolated teeth. **Layer 4:** one isolated tooth; one left upper M1.
554 **Layer 5:** two isolated teeth; one indeterminate and one left lower m1.

555 **Description and discussion:** as in other murines, the first upper molar (M1) has
556 three rows of tubercles: the first (t1, t2, t3) and second (t4, t5 and t6) groups
557 situated in the anterior part have three tubercles, and the third group (t7 and t9)
558 has two tubercles (Darviche et al., 2006). In Iran (Kryštufek and Vohralík, 2009)
559 both *Mus musculus domesticus* and *Mus macedonicus* may be found.

560 The specimens from Kaldar Cave fit well with *M. musculus* as regards the upper
561 M1 morphology: the lingual row of cusps (t1 and t4) is shifted posteriorly; cusp t7
562 is reduced to an enamel ridge; distal cusps t8 and t9 leave no space for a
563 posterior cingulum or posterolabial cusp t12 (Siahsarvie and Darvish, 2008). The
564 dental ends of the mesial and central cusps on m1 fuse early; the mesiolabial
565 cusp is small. Upper molars normally have three roots each, one lingual and two
566 labial, whereas lower molars are two-rooted (one anterior and one posterior)
567 (Kryštufek and Vohralík, 2009). Despite these observations, bearing in mind the
568 high intra-specific morphological variability, the low quantity of material and the
569 bad state of preservation of some teeth (Fig. 2.13), we only attribute the Kaldar
570 material to *M. cf. musculus*.

571 **Habitat and distribution:** *Mus musculus* is a commensal species, well
572 distributed throughout the world: it is present over all the continents except
573 Antarctica. It is found in a wide range of habitats but tends not to be found in
574 forest and deserts. *Mus musculus* is ecologically highly opportunistic but a weak
575 competitor; it can cope with aridity and can also expand into the desert (Kryštufek
576 and Vohralík, 2009). It is also found in arid habitats along the border with Syria
577 and Iraq, in desert landscapes and near the Euphrates River (Kryštufek &
578 Vohralík, 2009; Denys, 2017).

579 **4.2. Taphonomic remarks**

580 According to the different degrees of digestion (mostly light, moderate and, heavy
581 in a few cases) observed in the molars previously studied by one of the authors
582 (M. F.-G) and published in Bazgir et al. (2017), the predator responsible for this
583 accumulation could be a category 3 predator such as the tawny owl (*Strix aluco*)
584 or the Eurasian eagle owl (*Bubo bubo*). Both species are currently present in the
585 area, have opportunistic hunting habits, and are sedentary, so their prey
586 spectrum is assumed to be a good representation of the ecosystem in which they
587 live.

588 **4.3. Past landscape and climate at Kaldar Cave**

589 The small-mammal assemblages from Layers 4 and 5 of Kaldar Cave are
590 dominated by the genus *Microtus* (60 individuals in Layer 4 and 79 in Layer 5),

591 followed by *Ellobius* in Layer 4 (17 individuals) and *Meriones cf. persicus* (17
 592 individuals in Layer 4 and 18 in Layer 5). These species indicate that the
 593 environment in the area was mainly composed of open dry and steppe areas,
 594 although we also found *Apodemus sp.* and *Mus cf. musculus*, which are related
 595 rather to a dense vegetation cover (including trees/bush). All the species
 596 identified at Kaldar Cave still occur in the area today.

597 Layers 1-3 do not yield enough material to draw palaeoclimatic inferences (MNI
 598 < 30). For Layers 4 and 5, the *bioclimatic model* shows similar results (Table 6).
 599 It should be pointed out that some species are not included in the *BM* data matrix,
 600 such as *Myomimus* (present in Layer 4) and *Microtus guentheri* (Layer 5),
 601 because their values did not appear in the *BM* and could not be used in the
 602 analysis. The *BM* based on the small mammals from Kaldar Cave suggests lower
 603 temperatures and lower precipitation than at present in both Layers 4 and 5
 604 (Table 6). The MAT is around 6°C lower, and there is a higher temperature
 605 amplitude between maximum and minimum mean temperatures. This indicates
 606 that Layers 4 and 5 of Kaldar Cave were deposited during a colder period, which
 607 is not in agreement with the preliminary interpretations of Bazgir et al. (2017)
 608 suggesting a temperate “interstadial”.

	Layer 5	SD	Δ	Layer 4	SD	Δ	Current values
Mean annual temperature	10.90 °C	3.39	-6°C	11.73°C	3.39	-5.17°C	16.90 °C
Maximum mean temperature	23.45 °C	4.77	-6.15°C	23.10°C	4.77	-6.5°C	29.60 °C
Minimum mean temperature	-1.69 °C	4.66	-6.69°C	0.25°C	4.66	-4.75°C	5°C
Mean annual precipitation	258.68mm	533.24mm	-229.32mm	104.08mm	533.24mm	-383.92mm	488mm

609

610

611 Table 6: Bioclimatic model estimates for Kaldar Cave. SD, standard deviation. Δ
 612 (difference between the values obtained by analysing the rodents from Kaldar
 613 Cave and current values). Current values obtained from: [https://en.climate-
 614 data.org/asia/iran/lorestan/khorramabad-764550/](https://en.climate-data.org/asia/iran/lorestan/khorramabad-764550/)

615 The climate in Khorramabad nowadays is warm and temperate. The mean annual
 616 temperature is 16.9°C, the maximum mean temperature occurs in July with
 617 29.6°C and the minimum mean temperature is in January with 5°C
 618 (<https://en.climate-data.org/asia/iran/lorestan/khorramabad-764550/>). This
 619 contrast with the climactic conditions inferred from the *BM* on Kaldar Cave with
 620 lower temperatures and drier conditions. For layer 5, mean annual temperature is
 621 6°C lower than nowadays, the maximum mean temperature 6.15°C lower than
 622 the current values and the minimum mean temperature is 6.69°C lower than the
 623 extant temperatures; the mean annual precipitation is 229.32mm lower than at
 624 present. This tendency is also observable on the Layer 4 mean annual
 625 temperature is 5.17°C lower than at present, the maximum mean temperature
 626 6.5°C lower than nowadays and the minimum mean temperature is 4.75°C lower
 627 than the extant temperatures; the mean annual precipitation is 383.92mm lower
 628 than at present. (Table 6). Comparing both levels Layer 5 is slightly colder than
 629 Layer 4, and Layer 4 is drier than Layer 5.

630 Applying the *habitat weighting method*, our data show a palaeoenvironment
 631 mainly composed of steppes in both levels. In Layer 4, grasslands are also well
 632 represented, notably through the presence of *Microtus guentheri*. In Layer 5,
 633 deserts are the second most represented habitat, thanks to the considerable
 634 presence of *Myomimus* sp. The proportion of rocky areas is also significant,
 635 indicated by the presence of *Chionomys nivalis* and *Meriones* cf. *persicus* (Figure
 636 3).

637

638

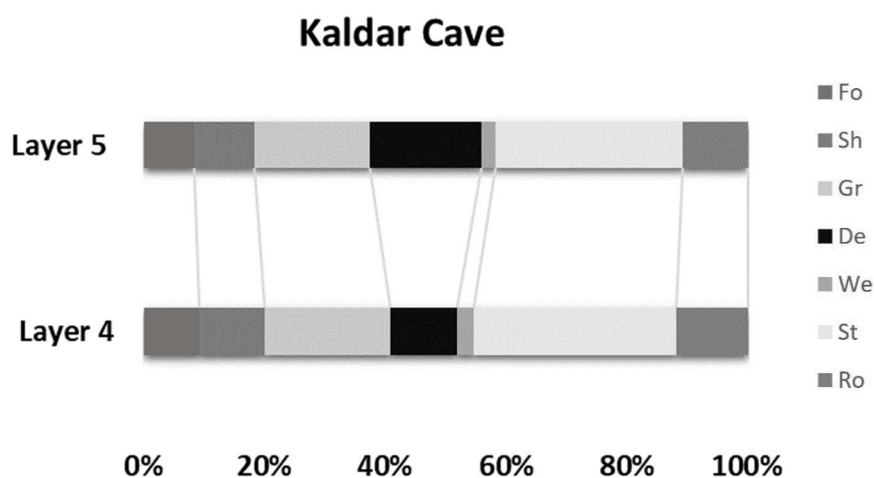
639

640

641

642

643



644 Figure 3: Results of the *habitat weighting method* for Kaldar Cave (Layer 4 and
645 Layer 5). Forest (Fo), Shrubland (Sh), Grassland (Gr), Desert (De), Wetland
646 (We), Steppe (St) and Rocky (Ro).

647

648 There thus seems to be no major palaeoenvironmental or palaeoclimatic change
649 that can explain the cultural shift between Layer 5 (Middle Palaeolithic) and 4
650 (Upper Palaeolithic). However, as also observed with the climatic parameters,
651 Layer 5 appears slightly colder and drier than Layer 4, with a higher proportion of
652 desert habitats.

653 We can compare these results with previous studies carried out in Kaldar Cave
654 using other palaeoenvironmental proxies. Charcoal analyses (Allué et al., 2018;
655 Bazgir et al., 2017) indicate that there were active water sources or flows, with
656 specific plant communities characteristic of open forest growing in cool and dry
657 conditions (Allué et al., 2018). The presence of forested areas is also supported
658 by the large mammals, with the presence of *Sus scrofa*, *Capreolus* sp. and
659 *Cervus elaphus* (Bazgir et al., 2017). Several amphibian and squamate species
660 have also been found (Bazgir et al., 2017): a toad (*Bufo* sp.), an agamid lizard
661 (Agamidae indet.), a gecko (Gekkonidae indet.), a skink (Scincidae indet.), a
662 lacertid (Lacertidae indet.), a glass lizard (*Pseudopus* sp.), a sand boa (*Eryx* sp.),
663 possibly six types of colubrine snakes (Colubrinae indet.), a cobra (Elapidae
664 indet.), and a viper (Viperidae indet.). Most of these taxa (Agamidae, *Eryx* and
665 Elapidae) live in savannahs, steppes and deserts, with a way of life always linked
666 with warm arid areas in rocky or sandy environments. *Pseudopus* lives in dry and
667 bushy environments, sometimes in open woodlands, but avoids dense forest
668 areas (Bazgir et al., 2017).

669 Our results based on small mammals, combined with previous studies of other
670 proxies, thus suggest a mosaic landscape alternating between dry-steppe areas
671 and wooded patches. Nowadays, the vegetation in the Zagros is a montane
672 grassland-woodland characterised by steppe of grassland and herbs with
673 occasional to fairly common trees. The principal local trees are deciduous oaks
674 and junipers, with maples, walnut, almond and ash at middle elevations, and

675 *Pistacia* and *Olea* in drier areas (Fiacconi and Hunt, 2015). Thus, the landscape
676 during the Middle and Upper Pleistocene at Kaldar Cave was similar to that today,
677 despite a colder climate.

678

679 **4.4. Kaldar Cave in the Middle Eastern context**

680 Kaldar Cave is situated in the Khorramabad Valley, which played a significant
681 role in human adaptation and dispersal during the Quaternary. Some other caves
682 close to Kaldar, such as Gilvaran, Ghamari and Gar Arjene rock shelter, have
683 yielded Mousterian and Aurignacian occupations (Bazgir et al., 2014). Moreover,
684 surveys in Kermanshah have also documented Middle and Upper Palaeolithic
685 sites (Heydari-Guran and Ghasidian, 2020). None of them has given rise to small-
686 mammal studies. However, Gilvaran Cave has been studied from a
687 palaeoenvironmental point of view through charcoal analyses (Allué et al., 2018),
688 showing a similar pattern to Kaldar, where *Prunus* is also present and indicates
689 the presence of open forest areas. Similarly, other proxies such as pollens and
690 charcoals have been analysed at Shanidar (Campana and Crabtree, 2019;
691 Fiacconi and Hunt, 2015) and Gilvaran (Allué et al., 2018), indicating similar
692 environmental conditions to Kaldar.

693 Other studies based on small mammals from the Middle East have been
694 performed in Qesem Cave (Maul et al., 2015a; Smith et al., 2015), Hummal (Maul
695 et al., 2015b), Azokh Cave (Fernández-Jalvo, 2016), Aghitu-3 Cave (Frahm,
696 2019; Kandel et al., 2017; Nishiaki and Akazawa, 2018), Neshar Ramla
697 (Weissbrod and Zaidner, 2014), Amud Cave (Belmaker and Hovers, 2011),
698 Dzudzuana Cave (Belmaker et al., 2016) and Karain Cave (Demirel et al., 2011).
699 These studies did not use *HW* or the *BM* for their palaeoclimatic and
700 palaeoenvironmental reconstructions, and the sites are not always contemporary
701 with Kaldar, except Amud Cave (Belmaker and Hovers, 2011), Aghitu-3 (Djamali
702 et al., 2008; Kandel et al., 2017) and Dzudzuana Cave (Belmaker et al., 2016)
703 (Table 7).

704

705

Site/Author	Layer	Human culture	Chronology	Environmental conditions	Rodent
Amud Cave (Belmaker and Hovers, 2011)	B4	Neanderthals	68.5 ± 3.4ka	Grassland vegetation	<i>Microtus guentheri</i>
	B2-B1	Neanderthals	56.5 ± 3.5, 57.6 ± 3.7, respectively	Woodland	<i>Apodemus cf. mystacinus</i> and <i>Mus macedonicus</i>
Dzudzuana Cave (Belmaker et al., 2016)	Unit C	Modern human	27-24ka cal BP	Mild and humid	<i>Microtus, Ellobius, Arvicola, Apodemus</i> and <i>Allactaga</i> .
Aghitu-3 (Djamali et al., 2008; Kandel et al., 2017)	Level VII-III	Modern human	The oldest layer is VII with a chronology between 39-36,000 cal BP and the most recent is layer III, between 29-24,000 cal BP	This sequence documents that the climate becomes colder	<i>Microtus spp., Chionomys sp., Arvicola amphibius</i> and <i>Ellobius lutescens</i>

706 Table 7: Comparison between Middle Eastern sites with small-mammal studies

707

708 Most of these studies highlight problems in identifying Middle Eastern rodent
709 species, as faced in the present work. There are some studies of present-day
710 taxonomy and systematics in Iran, Turkey, Israel, Jordan, Lebanon and Syria
711 (Abi-said et al., 2014; Darvish et al., 2000; Haddadian Shad et al., 2014; Kopij
712 and Liven-schulman, 2013; Obuch and Khaleghizadeh, 2012; Shehab et al.,
713 2013), but these are mostly based on skull morphology and thus not applicable
714 in archaeological or palaeontological contexts where the remains are broken.
715 Very few studies provide descriptions of molars with comparative elements,
716 allowing for the correct identification of fossil specimens. In this context,
717 comparison with modern specimens from museum collections of genetically
718 typed specimens is crucial to establish a correct taxonomic reference.

719 Palaeoenvironmental inferences have been drawn on the basis of small-mammal
720 studies, as well as palynological and anthracological analyses. During the Upper
721 Pleistocene, small-mammal compositions differ from one site to another
722 (Belmaker et al., 2016; Kandel et al., 2017) (Table 8), probably because the sites
723 are not exactly contemporaneous and are likely to belong to different eco-regions.
724 It is noteworthy that the genera *Microtus*, *Chionomys*, *Cricetulus*, *Mesocricetus*,

725 *Ellobius* and *Allactaga* are represented in all the sites, allowing us to reconstruct
 726 the species communities of this region. Kaldar is the most diverse site in terms of
 727 small-mammal species.

728

Taxon	Kaldar Cave			Aghitu-3			Dzudzuana	
	Layers 1-3	Layer 4	Layer 5	VII	VI	V-IV	III	Unit C
<i>Microtus</i> spp.	X	X	X	X	X	X	X	
<i>Microtus</i> cf. <i>arvalis</i>								X
<i>Microtus irani</i>	X		X					
<i>Microtus guentheri</i>	X	X						
<i>Microtus socialis</i>	X	X	X					
<i>Chionomys nivalis</i>	-	X	X	X	X	X	X	X
<i>Clethrionomys glareolus</i>								X
<i>Ellobius</i> spp.	X	X	X					
<i>Ellobius fuscocapillus</i>	X	X	X					
<i>Ellobius lutescens</i>	-	X	X	X				X
<i>Cricetus cricetus</i>								X
<i>Cricetulus migratorius</i>	X	X	X	X		X	X	X
<i>Mesocricetus brandti</i>		X	X	X	X	X	X	X
<i>Meriones</i> cf. <i>persicus</i>	X	X	X					
<i>Allactaga</i> sp.		X	X	X	X		X	X
<i>Myomimus</i> sp.			X					
<i>Apodemus</i> sp.	X	X	X					X
<i>Mus musculus</i>		X	X					X
<i>Arvicola amphibius</i>				X	X	X	X	X

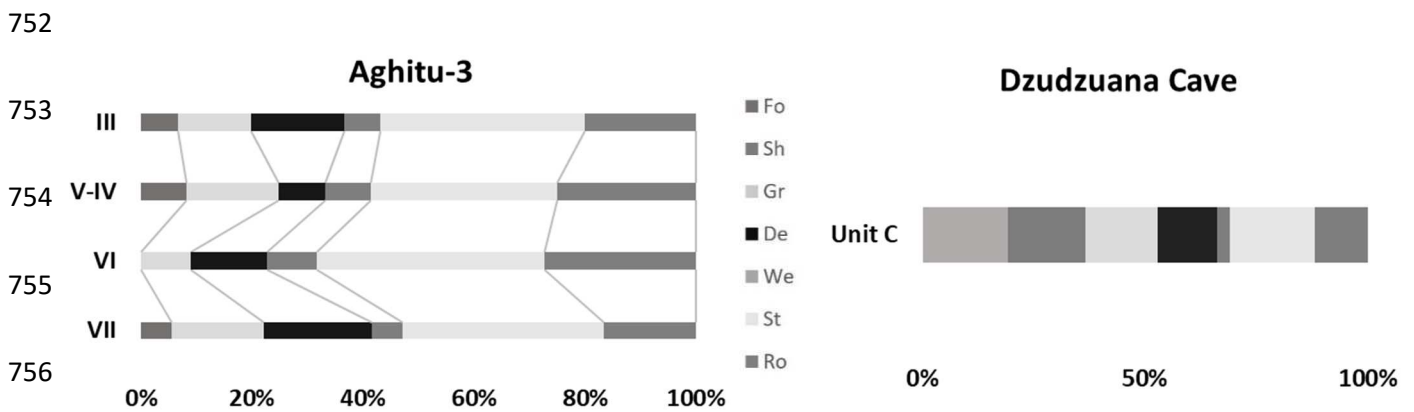
729 Table 8: comparison of the small-mammal lists from several Upper Palaeolithic
 730 sites in the Middle East.

731

732 We applied the *habitat weighting method* at other Middle Eastern sites where
 733 small-mammal studies have been performed, namely Aghitu-3 and Dzudzuana
 734 Cave, but these are located in other eco-regions (Figure 1a). Aghitu-3 is located
 735 in Armenian Highlands (46°08'22" E, 39°51'38" N), at an elevation of 1601 m a.s.l.
 736 and the current climate is continental with considerable seasonality in
 737 temperature. Dzudzuana Cave is located in Georgian Caucasus foothills
 738 (43°06'11" E, 42°13'27" N), at an elevation of 560 m a.s.l., and the current climate
 739 is warm and temperate. The estimations obtained with the *habitat weighting*
 740 *method* (Figure 4) show similar environmental conditions between Kaldar Cave
 741 and Aghitu-3, where the landscape is dominated by steppe (indicated by the

742 presence of *Ellobius lutescens*, *Mesocricetus brandti*, *Cricetulus migratorius* and
 743 *Allactaga*), with a relatively high percentage of grassland and forests.

744 To ascertain the palaeoclimatic conditions, we calculated and directly compared
 745 our results with Aghitu-3 and Dzudzuana Cave using the *bioclimatic method*
 746 (Table 9). The results obtained for Aghitu-3 show higher temperatures and
 747 precipitation than at present, whereas Dzudzuana Cave shows the same pattern
 748 as Kaldar Cave, with drier conditions and lower temperatures than today. For
 749 Amud Cave, it was not possible to calculate *HW* and *BM*, but data from the
 750 literature (Belmaker and Hovers, 2011) indicate a grassland environment similar
 751 to the one that we reconstructed at Dzudzuana Cave.



757

758

759 Figure 4: Results of the *habitat weighting method* for Aghitu-3 and Dzudzuana
 760 Cave. Forest (Fo), Shrubland (Sh), Grassland (Gr), Desert (De), Wetland (We),
 761 Steppe (St) and Rocky (Ro).

	<u>Aghitu-3</u>					Current Values	<u>Dzudzuana Cave</u>		Current Values
	VII	VI	V-IV	III	SD		Unit C	SD	
Mean annual Temperature	15.46 °C	19.44 °C	19.21 °C	17.87 °C	3.386	8.5 °C	5.09 °C	3.39	9.7 °C
Maximum mean temperature	23.59 °C	24.44 °C	24.09 °C	24 °C	4.772	20.2 °C	18.55 °C	4.77	20.3 °C
Minimum mean temperature	7.31 °C	14.67 °C	14.72 °C	11.96 °C	4.656	-3.8 °C	-8.26 °C	4.66	-1.6 °C
Mean annual precipitation	1169.04 mm	1729.48 mm	1825.99 mm	1484.60 mm	533.236	532 °C	194.98mm	533.24	868mm

762 Table 9: Estimates using the *bioclimatic method* for Aghitu-3 and Dzudzuana
763 Cave. SD, standard deviation. Current values obtained from Kandel et al. (2017)
764 for Aghitu-3 and [https://es.climate-data.org/asia/georgia/imereti/jria-
765 414325/?amp=true](https://es.climate-data.org/asia/georgia/imereti/jria-414325/?amp=true) for Dzudzuana Cave.

766 **5. Conclusions**

767 This work represents the first study of a Late Pleistocene rodent assemblage from
768 the Middle East with palaeoenvironmental and palaeoclimatic reconstructions,
769 using and adapting the *habitat weighting method* and the *bioclimatic model* to this
770 area. We identified 1112 rodent remains, corresponding to a minimum number of
771 264 individuals. The rodent assemblage is composed of 13 taxa: six arvicoline
772 (*Microtus socialis*, *Microtus irani*, *Microtus guentheri*, *Chionomys nivalis*, *Ellobius*
773 *fuscocapillus* and *Ellobius lutescens*), two cricetine (*Cricetulus migratorius* and
774 *Mesocricetus brandti*), one glirid (*Myomimus* sp.), one gerbilline (*Meriones* cf.
775 *persicus*), one dipodid (*Allactaga* sp.) and two murine species (*Apodemus* sp.
776 and *Mus* cf. *musculus*). Augmenting the preliminary analysis of the material
777 (Bazgir et al., 2017), new species were identified, such as *Microtus socialis*,
778 *Microtus irani*, *Microtus guentheri*, *Ellobius fuscocapillus* and *Meriones* cf.
779 *persicus*. We also reconsidered the identification of *Ellobius talpinus*,
780 *Calomyscus* sp. and *Dryomys* cf. *nitedula*, based on modern specimens from
781 museum collections and measurements; this is why they do not appear in the
782 new faunal list of Kaldar Cave.

783 Given the scarcity of studies in this biogeographical region, we encountered some
784 difficulties in the identification of species, which could slightly affect the
785 palaeoenvironmental and palaeoclimatic interpretations. In order to counter these
786 potential errors, further studies of small mammals in this region are necessary,
787 as well as research on discriminant characters in molars, using reference
788 collections including genetically typed specimens.

789 The palaeoecological analysis of the rodents from Kaldar Cave revealed lower
790 temperatures and lower precipitation than present-day conditions, and an
791 environment mainly composed of dry steppes with patches of forested areas. The
792 results obtained are supported by palynological, anthracological and large-

793 mammal studies. At a broader geographical scale, colder conditions were also
794 inferred at Dzudzuana Cave. The genera *Microtus*, *Chionomys*, *Cricetulus*,
795 *Mesocricetus*, *Ellobius* and *Allactaga* are present at all the Middle East sites
796 (Aghitu-3, Dzudzuana and Amud) during the Upper Pleistocene, that have
797 yielded small mammals, allowing us to reconstruct the rodent communities of the
798 area.

799 Considering all the results from Kaldar Cave and other contemporaneous sites,
800 we can conclude that both Neanderthals and AMH lived in dry steppes with
801 patches of forested areas, without major environmental changes occurring
802 between the Middle and the Late Palaeolithic. Climatic shifts during the MIS 4-3
803 transition were of a magnitude that did not have a major impact on small
804 mammals in the region, suggesting that climate change may not have had the
805 hypothesized effect on the Neanderthal extinction in the Levant.

806 **Acknowledgments:** I. Rey-Rodriguez is the beneficiary of a PhD scholarship
807 funded by the Erasmus Mundus Program (IDQP). J.M. López-García was
808 supported by a Ramón y Cajal contract (RYC-2016-19386) with financial
809 sponsorship from the Spanish Ministry of Science, Innovation and Universities.
810 M. Fernández-García is the beneficiary of a PEJ grant (PEJ2018-005222-P)
811 funded by the Spanish National Youth Guarantee System and the European
812 Social Fund. This work was developed within the framework of the projects
813 2017SGR859, 2017SGR840 and 2017SGR1040 (AGAUR, Generalitat de
814 Catalunya), and 2018PFRURVB291 (Univ. Rovira i Virigli). We thank the head of
815 the Research Institute of Cultural Heritage and Tourism (RICHT) (Dr. B. Omrani)
816 and the head of the Iranian Center for Archaeological Research (ICAR) (Dr. R.
817 Shirazi) for providing us with the necessary support and permissions in studying
818 the materials. We thank the head of the Lorestan Cultural Heritage, Handicraft
819 and Tourism Organization (Mr. A. Ghasemi) for all his support. We also thank the
820 head of International Collaboration and Ties of the RICHT (Mrs. M. Kholghi) for
821 all her cooperation and help. B. Bazgir received his PhD scholarship from the
822 Fundación Atapuerca, for which he is grateful. Laxmi Tumung received her PhD
823 scholarship from the Erasmus Mundus Programme (IDQP). We would like to
824 thank Roberto Portela Miguez, Senior Curator in Charge of Mammals, for his help
825 with the reference collection in the Natural History Museum of London. We would

826 like to thank Rupert Glasgow for reviewing the English language of the
827 manuscript. We also want to thank to the Editor Prof.
828 José S. Carrión and the two anonymous reviewer for their comments and
829 suggestions that strongly improve the final version of the manuscript.

830 **References**

- 831 Abi-Said, M.R., Shehab, A.H., Amr, Z.S., 2014. Diet of the Barn Owl. Jordan
832 Journal of Biological Sciences, Vol. 7, Nº 2, 109–112.
- 833 Allué, E., Expósito, I., Tumung, L., Ollé, A., Bazgir, B., 2018. Early evidence of
834 *Prunus* and *Prunus* cf. *amygdalus* from Palaeolithic sites in the
835 Khorramabad Valley, western Iran. *Comptes Rendus Palevol* 17, 335–345.
836 <https://doi.org/10.1016/j.crpv.2018.01.001>
- 837 Amori, G. 1999. *Chionomys nivalis*. In: A. J. Mitchell-Jones, G. Amori, W.
838 Bogdanowicz, B. Kryštufek, P. J. H. Reijnders, F. Spitzenberger, M.
839 Stubbe, J. B. M. Thissen, V. Vohralík and J. Zima (eds), *The Atlas of*
840 *European Mammals*, Academi Press, London, UK
- 841 Amori, G., Hutterer, R., Kryštufek, B., Yigit, N., Mitsain, G. & Palomo, L.J., 2016.
842 *Apodemus flavicollis*. The IUCN Red List of Threatened Species 2016:
843 e.T1892A115058023. 8235.
844 [https://doi.org/http://dx.doi.org/10.2305/IUCN.UK.2016-](https://doi.org/http://dx.doi.org/10.2305/IUCN.UK.2016-3.RLTS.T1892A22423256.en)
845 [3.RLTS.T1892A22423256.en](https://doi.org/http://dx.doi.org/10.2305/IUCN.UK.2016-3.RLTS.T1892A22423256.en)
- 846 Amr, A., 2015. *Microtus guentheri*. The IUCN Red List of Threatened
847 Species 2016: e.T13463A22349143.
- 848 Andrews, P., 1990. Owls, Caves and Fossils. <https://doi.org/10.2307/3889096>
- 849 Andrews, P., 2006. Taphonomic effects of faunal impoverishment and faunal
850 mixing. *Palaeogeography, Palaeoclimatology, Palaeoecology* 241, 572–
851 589. <https://doi.org/10.1016/j.palaeo.2006.04.012>
- 852 Aşan Baydemir, N., Duman, L., 2009. Molar patterns in *Microtus guentheri*
853 (Danford and Alston, 1880) (Mammalia: Rodentia) from Kirikkale province.
854 *Journal of Applied Biological Sciences* 3, 47–54.
- 855 Bazgir, B., Ollé, A., Tumung, L., Becerra-Valdivia, L., Douka, K., Higham, T.,

856 Van Der Made, J., Picin, A., Saladié, P., López-García, J.M., Blain, H.-A.,
857 Allué, E., Fernández-García, M., Rey-Rodríguez, I., Arceredillo, D.,
858 Bahrololoumi, F., Azimi, M., Otte, M., Carbonell, E., 2017. Understanding
859 the emergence of modern humans and the disappearance of Neanderthals:
860 Insights from Kaldar Cave (Khorramabad Valley, Western Iran). *Scientific*
861 *Reports* 7. <https://doi.org/10.1038/srep43460>

862 Bazgir, B., Otte, M., Tumung, L., Ollé, A., Deo, S.G., Joglekar, P., López-
863 García, J.M., Picin, A., Davoudi, D., van der Made, J., 2014. Test
864 excavations and initial results at the middle and upper paleolithic sites of
865 Gilvaran, Kaldar, Ghamari caves and Gar Arjene Rockshelter,
866 Khorramabad Valley, western Iran. *Comptes Rendus - Palevol* 13, 511–
867 525. <https://doi.org/10.1016/j.crpv.2014.01.005>

868 Becerra-Valdivia, L., Douka, K., Comeskey, D., Bazgir, B., Conard, N.J.,
869 Marean, C.W., Ollé, A., Otte, M., Tumung, L., Zeidi, M., Higham, T.F.G.,
870 2017. Chronometric investigations of the Middle to Upper Paleolithic
871 transition in the Zagros Mountains using AMS radiocarbon dating and
872 Bayesian age modelling. *Journal of Human Evolution* 109, 57–69.
873 <https://doi.org/10.1016/j.jhevol.2017.05.011>

874 Belmaker, M., Bar-Yosef, O., Belfer-Cohen, A., Meshveliani, T., Jakeli, N.,
875 2016. The environment in the Caucasus in the Upper Paleolithic (Late
876 Pleistocene): Evidence from the small mammals from Dzudzuana cave,
877 Georgia. *Quaternary International* 425, 4–15.
878 <https://doi.org/10.1016/j.quaint.2016.06.022>

879 Belmaker, M., Hovers, E., 2011. Ecological change and the extinction of the
880 Levantine Neanderthals: Implications from a diachronic study of
881 micromammals from Amud Cave, Israel. *Quaternary Science Reviews* 30,
882 3196–3209. <https://doi.org/10.1016/j.quascirev.2011.08.001>

883 Blain, H.-A., Bailon, S., Cuenca-Bescós, G., 2008. The Early–Middle
884 Pleistocene palaeoenvironmental change based on the squamate reptile
885 and amphibian proxies at the Gran Dolina site, Atapuerca, Spain.
886 *Palaeogeography, Palaeoclimatology, Palaeoecology* 261, 177–192.
887 <https://doi.org/10.1016/j.palaeo.2008.01.015>

- 888 Bogicevic, K., Nenadic, D., Mihailovic, D., Lazarevic, Z., Milivojevic, J., 2011.
889 Late Pleistocene rodents (Mammalia: Rodentia) from the Baranica cave
890 near Knjaževac (eastern Serbia): Systematics and palaeoecology. *Rivista*
891 *Italiana di Paleontologia e Stratigrafia*, Vol. 117, N°2, 331-346.
- 892 Campana, D. V., Crabtree, P., 2019. Evidence for skinning and craft activities
893 from the Middle Paleolithic of Shanidar Cave, Iraq. *Journal of*
894 *Archaeological Science: Reports* 25, 7–14.
895 <https://doi.org/10.1016/j.jasrep.2019.03.024>
- 896 Corbet, G.B., 1978. *The Mammals of the Palearctic Region: A Taxonomic*
897 *Review*. London, Brit. Mus.(Nat. Hist.). Cornell Univ. Press. 117- 118.
- 898 Corbet, G.B. and Hill, J.E., 1991. *A World List of Mammalian Species*. 3rd ed.
899 London, UK: British Museum (Natural History).
- 900 Coşkun, Y., 2016. Review of unique odd chromosome-numbered underground
901 rodent species of the Palearctic region: *Ellobius Lutescens* Thomas 1897
902 (Rodentia: Cricetidae). *Turkish Journal of Zoology* 40, 831–841.
903 <https://doi.org/10.3906/zoo-1509-53>
- 904 Coşkun, Y., 1999. Morphological characteristics of *Meriones tristrami* Thomas,
905 1892 (Rodentia: Gerbillinae) from Diyarbakır, Turkey. *Turk. J. Zool* 23,
906 345–355.
- 907 Coşkun, Y., 1997. *Ellobius lutescens* Thomas, 1897 (Rodentia: Cricetidae) *Turk.*
908 *J. of Zoology*. 21, 349-354.
- 909 Darlington, P.J., 1957. *Zoogeography: The Geographical Distribution of*
910 *Animals*. New York, NY, USA: John Wiley and Sons.
- 911 Darviche, D., Orth, A., Michaux, J., 2006. *Mus spretus* et *M. musculus*
912 (Rodentia, Mammalia) en zone méditerranéenne: Différenciation
913 biométrique et morphologique: Application à des fossiles marocains
914 pléistocènes. *Mammalia* 70, 90–97.
915 <https://doi.org/10.1515/MAMM.2006.010>
- 916 Darvish, J., Mohammadi, Z., Mahmoudi, A., Siah sarvie, R., 2014. Faunistic and
917 taxonomic study of Rodents from northwestern Iran. *Iranian Journal of*

- 918 Animal Biosystematics (IJAB) 10, 119–136.
- 919 Darvish, J., 2011. Morphological comparison of fourteen species of the genus
920 *Meriones* Illiger , 1811 (Rodentia : Gerbillinae) from Asia and North Africa.
921 Iranian Journal of Animal Biosystematics 7, 49–74.
- 922 Darvish, J., Ghiyasi, R., Khosravi, M., 2000. Recognition of rodents of Robat
923 Sharaf pellets owl by morphological and neontological studies. Journal of
924 Sciences 12.
- 925 Denys, C., 2017. Subfamily Deomyinae, Gerbillinae, Leimacomyinae,
926 Lophiomyinae species accounts. Pp. 598-650. in : Wilson, D.E., Lacher,
927 T.E., Jr. & Mittermeier, R.A. eds. Handbook of the Mammals of the World.
928 Vol.7. Rodents II. Lynx Edicions, Barcelona.
- 929 Demirel, A., Andrews, P., Yalçinkaya, I., Ersoy, A., 2011. The taphonomy and
930 palaeoenvironmental implications of the small mammals from Karain Cave,
931 Turkey. Journal of Archaeological Science 38, 3048–3059.
932 <https://doi.org/10.1016/j.jas.2011.07.003>
- 933 Dianat, M., Darvish, J., Cornette, R., Aliabadian, M., Nicolas, V., 2017.
934 Evolutionary history of the Persian Jird, *Meriones persicus*, based on
935 genetics, species distribution modelling and morphometric data. Journal of
936 Zoological Systematics and Evolutionary Research 55, 29–45.
937 <https://doi.org/10.1111/jzs.12145>
- 938 Djamali, M., de Beaulieu, J.L., Shah-hosseini, M., Andrieu-Ponel, V., Ponel, P.,
939 Amini, A., Akhiani, H., Leroy, S.A.G., Stevens, L., Lahijani, H., Brewer, S.,
940 2008. A late Pleistocene long pollen record from Lake Urmia, NW Iran.
941 Quaternary Research 69, 413–420.
942 <https://doi.org/10.1016/j.yqres.2008.03.004>
- 943 Ellerman, J.R, and Morrison-Scott, T.C.S., 1951. Checklist of Palearctic and
944 Indian Mammals, 1780 to 1946. Brit. Mus. Nat. Hist. London, 1-810.
- 945 Evans, E.M.N., Van Couvering, J.A.H., Andrews, P., 1981. Palaeoecology of
946 Miocene sites in western Kenya. J. Hum. Evol. 10, 99-116.
- 947 Fernández-Jalvo Y., King T., Yepiskoposyan L. & Andrews P. (eds.), 2016a.

- 948 Azokh Cave and the Transcaucasian Corridor, Vertebrate Paleobiology and
949 Paleanthropology Series, Springer
- 950 Fernández-Jalvo, Y., Andrews, P., Denys, C., Sesé, C., Stoetzel, E., Marin-
951 Monfort, D., Pesquero, D., 2016b. Taphonomy for taxonomists: Implications
952 of predation in small mammal studies. *Quaternary Science Reviews* 139,
953 138–157. <https://doi.org/10.1016/j.quascirev.2016.03.016>
- 954 Fiacconi, M., Hunt, C.O., 2015. Pollen taphonomy at Shanidar Cave (Kurdish
955 Iraq): An initial evaluation. *Review of Palaeobotany and Palynology* 223,
956 87–93. <https://doi.org/10.1016/j.revpalbo.2015.09.003>
- 957 Firouz, E., 2005. *The complete fauna of Iran*. Ed. I.B.Tauris & Co Ltd
- 958 Frahm, E., 2019. Upper Palaeolithic Settlement and Mobility in the Armenian
959 Highlands : Agent-Based Modeling , Obsidian Sourcing , and Lithic
960 Analysis at Aghitu-3 Cave.
- 961 Gerrie, R., Kennerley, R., 2017. *Myomimus personatus*. The IUCN Red List of
962 Threatened Species 2017: e.T14088A22222124 8235.
963 [https://doi.org/http://dx.doi.org/10.2305/IUCN.UK.2017-](https://doi.org/http://dx.doi.org/10.2305/IUCN.UK.2017-2.RLTS.T14088A22222124.en)
964 [2.RLTS.T14088A22222124.en](https://doi.org/http://dx.doi.org/10.2305/IUCN.UK.2017-2.RLTS.T14088A22222124.en)
- 965 Gharkheloo, M., Kivanç, E., 2003, A study on the morphology, karyology and
966 distribution of *Ellobius* Fischer, 1814 (Mammalia: Rodentia) in Iran. *Turkish*
967 *Journal of Zoology* 27(4):281-292
- 968 Golenishchev, F.,Malikov, V., Nazari, F., Vaziri, A.,Sablina, O., Polyakov, A.,
969 2002. New species of vole of “*guentheri*“ group (Rodentia, Arvicolinae,
970 *Microtus*) from Iran. *Russia Journal of Theriology* 1 (2), 117-123
- 971 Golenishchev, F., Malikov, V., Petrova, T., Bodrov, S., Abramson, N., 2019.
972 Toward assembling a taxonomic puzzle: Case study of Iranian gray voles
973 of the subgenus *Microtus* (Rodentia, Cricetidae). *Mammalian Biology* 94,
974 98–105. <https://doi.org/10.1016/j.mambio.2018.06.007>
- 975 Habibi, K. 2004. *Mammals of Afghanistan*. Zoo Outreach Organisation/USFWS,
976 Coimbatore, India.
- 977 Haddadian Shad, H., Darvish, J., Mohammadian, T., Mahmoudi, A., Alaie

- 978 Kakhki, N., Ghanbarifardi, M., Molavi, F., Barani-Beiranvand, H., 2014.
979 Preliminary study of rodents using pellets of predatory birds in Iran. Iranian
980 Journal of Animal Biosystematics 10, 36–50.
- 981 Hassinger, J.D., 1973. A survey of the mammals of Afghanistan: Resulting from
982 the 1965 Street Expedition (Excluding Bats). Fieldiana Zoology, Vol. 60.
983 Chicago, IL, USA: Field Museum of Natural History.
- 984 Hernández Fernández, M., 2001. Bioclimatic discriminant capacity of terrestrial
985 mammal faunas. Global Ecology and Biogeography 10, 189–204.
986 <https://doi.org/10.1046/j.1466-822x.2001.00218.x>
- 987 Hernandez Fernández, M., Peláez-Campomanes, P., 2003. The bioclimatic
988 model: A method of palaeoclimatic qualitative inference based on mammal
989 associations. Global Ecology and Biogeography 12, 507–517.
990 <https://doi.org/10.1046/j.1466-822X.2003.00057.x>
- 991 Hernández Fernández, M., Álvarez Sierra, M.Á., Peláez-Campomanes, P.,
992 2007. Bioclimatic analysis of rodent palaeofaunas reveals severe climatic
993 changes in Southwestern Europe during the Plio-Pleistocene.
994 Palaeogeography, Palaeoclimatology, Palaeoecology 251, 500–526.
995 <https://doi.org/10.1016/j.palaeo.2007.04.015>
- 996 Heydari-Guran, S., Ghasidian, E., 2020. Late Pleistocene hominin settlement
997 patterns and population dynamics in the Zagros Mountains : Kermanshah
998 region. Archaeological Research in Asia 21, 100161.
999 <https://doi.org/10.1016/j.ara.2019.100161>
- 1000 Hinton, M.A.C., 1926. Monograph of the Voles and Lemmings (Microtinae)
1001 Living and Extinct. London: British Museum (Natural History). Vol.1. 488 p.
- 1002 Jangjoo, M., J.Darvish & J. D. Vign 2011. Application of outline analysis on
1003 fossil and modern specimens of *Apodemus*. – Iranian J. Anim. Biosystem.,
1004 7 (2): 143-155.
- 1005 Kandel, A.W., Gasparyan, B., Allué, E., Bigga, G., Bruch, A.A., Cullen, V.L.,
1006 Frahm, E., Ghukasyan, R., Gruwier, B., Jabbour, F., Miller, C.E., Taller, A.,
1007 Vardazaryan, V., Vasilyan, D., Weissbrod, L., 2017. The earliest evidence
1008 for Upper Paleolithic occupation in the Armenian Highlands at Aghitu-3

- 1009 Cave. *Journal of Human Evolution* 110, 37–68.
1010 <https://doi.org/10.1016/j.jhevol.2017.05.010>
- 1011 Karami, M., Hutterer, R., Benda, P., Siahsarvie, R., Kryštufek, B., 2008.
1012 Annotated check-list of the mammals of Iran. *Lynx (Praha)* 39, 63–102.
- 1013 Kaya, F., Kaymakçı, N., 2018. Systematics and dental microwear of the late
1014 Miocene Gliridae (Rodentia, Mammalia) from Hayranlı, Anatolia:
1015 Implications for paleoecology and paleobiodiversity. *Palaeontologia*
1016 *Electronica* 16. <https://doi.org/10.26879/385>
- 1017 Kennerley, R., Kryštufek, B., 2019. *Myomimus setzeri*. The IUCN Red List of
1018 Threatened Species 2019: e.T14089A22222049. 8235.
1019 [https://doi.org/http://dx.doi.org/10.2305/IUCN.UK.2019-](https://doi.org/http://dx.doi.org/10.2305/IUCN.UK.2019-1.RLTS.T14089A22222049.en)
1020 [1.RLTS.T14089A22222049.en](https://doi.org/http://dx.doi.org/10.2305/IUCN.UK.2019-1.RLTS.T14089A22222049.en)
- 1021 Knitlová, M., Horáček, I., 2017. Late Pleistocene-Holocene paleobiogeography
1022 of the genus *Apodemus* in Central Europe. *PLoS ONE* 12, 1–23.
1023 <https://doi.org/10.1371/journal.pone.0173668>
- 1024 Kopij, G., Liven-Schulman, I., 2013. Zoology in the Middle East Diet of the
1025 Lesser Kestrel, *Falco naumanni*, in Israel 7140.
1026 <https://doi.org/10.1080/09397140.2012.10648914>
- 1027 Kretzoi, M., 1969. Skizze einer Arvicoliden Phylogenie -Stand 1969 //
1028 *Vertebrata Hungarica*. Vol.11. No.1–2. P.155–193.
- 1029 Kryštufek, B., Bukhnikashvili, A., Sozen, M., Isfendiyaroglu, S., 2017. *Cricetulus*
1030 *migratorius*. The IUCN Red List of Threatened Species 2016:
1031 e.T5528A115073390 8235.
1032 [https://doi.org/http://dx.doi.org/10.2305/IUCN.UK.2016-](https://doi.org/http://dx.doi.org/10.2305/IUCN.UK.2016-3.RLTS.T5528A22391440.en)
1033 [3.RLTS.T5528A22391440.en](https://doi.org/http://dx.doi.org/10.2305/IUCN.UK.2016-3.RLTS.T5528A22391440.en)
- 1034 Kryštufek, B., Yigit, N., Amori, G., 2015. *Mesocricetus brandti*, Brandt ' s
1035 Hamster. The IUCN Red List of Threatened Species 2008:
1036 e.T13220A3421550. 8235.
1037 [https://doi.org/http://dx.doi.org/10.2305/IUCN.UK.2008.RLTS.T13220A3421](https://doi.org/http://dx.doi.org/10.2305/IUCN.UK.2008.RLTS.T13220A3421550.en)
1038 [550.en](https://doi.org/http://dx.doi.org/10.2305/IUCN.UK.2008.RLTS.T13220A3421550.en)

- 1039 Kryštufek, B. , Shenbrot, G., 2016. *Ellobius lutescens* , Transcaucasian Mole
1040 Vole. The IUCN Red List of Threatened Species 2016: e.T7655A22340006.
1041 8235. <https://doi.org/http://dx.doi.org/10.2305/IUCN.UK.2016->
1042 2.RLTS.T7655A22340006.en
- 1043 Krystufek, B., 2017. *Chionomys nivalis* , European Snow Vole. The IUCN Red
1044 List of Threatened Species 2016: e.T4659A115069366 8235.
1045 <https://doi.org/http://dx.doi.org/10.2305/IUCN.UK.2016->
1046 3.RLTS.T4659A22379147.en
- 1047 Kryštufek, B., Kefelioğlu, H., 2001. Redescription and species limits of *Microtus*
1048 *irani* Thomas, 1921, and description of a new social vole from Turkey
1049 (Mammalia: Arvicolinao).
- 1050 Kryštufek, B., Vohralík, V., 2009. Mammals of Turkey and Cyprus, Rodentia II:
1051 Cricetinae, Muridae, Spalacidae, Calomyscidae, Capromyidae, Hystricidae,
1052 Castoridae. <https://doi.org/10.1644/10-MAMM-R-221.1>
- 1053 Lay, D.M., 1967. A Study of the Mammals of Iran, Resulting from the Street
1054 Expedition of 1962-63. *Fieldiana Zool.*, 54: 168-171.
- 1055 López-García, J.M., 2011. Los micromamíferos del Pleistoceno superior de la
1056 Península Ibérica: Evolución de la diversidad taxonómica y cambios
1057 paleoambientales y paleoclimáticos. Editorial Académica Española
- 1058 López-García, J.M., Blain, H.-A., Cuenca-Bescós, G., Alonso, C., Alonso, S.,
1059 Vaquero, M., 2011. Small vertebrates (Amphibia, Squamata, Mammalia)
1060 from the late Pleistocene-Holocene of the Valdavara-1 cave (Galicia,
1061 northwestern Spain). *Geobios* 44, 253–269.
1062 <https://doi.org/10.1016/j.geobios.2010.10.001>
- 1063 Maul, L.C., Bruch, A.A., Smith, K.T., Shenbrot, G., Barkai, R., Gopher, A.,
1064 2015a. Palaeoecological and biostratigraphical implications of the
1065 microvertebrates of Qesem Cave in Israel. *Quaternary International*.
1066 <https://doi.org/10.1016/j.quaint.2015.04.032>
- 1067 Maul, L.C., Smith, K.T., Shenbrot, G., Bruch, A.A., Wegmüller, F., Le Tensorer,
1068 J.M., 2015b. Microvertebrates from unit G/layer 17 of the archaeological
1069 site of Hummal (El Kowm, Central Syria): Preliminary results. *Anthropologie*

- 1070 (France) 119, 676–686. <https://doi.org/10.1016/j.anthro.2015.10.010>
- 1071 Miller, G.S., 1896. Genera and subgenera of voles and lemmings// North
1072 American Fauna. Vol.12. P.1–85.
- 1073 Molur, S. & Sozen, M., 2016. *Meriones persicus*, Persian Jird. The IUCN Red
1074 List of Threatened Species 2016: e.T13166A22433231. 8235.
1075 [https://doi.org/http://dx.doi.org/10.2305/IUCN.UK.2016-](https://doi.org/http://dx.doi.org/10.2305/IUCN.UK.2016-2.RLTS.T13166A22433231.en)
1076 [2.RLTS.T13166A22433231.en](https://doi.org/http://dx.doi.org/10.2305/IUCN.UK.2016-2.RLTS.T13166A22433231.en)
- 1077 Moradi Gharkheloo, M., 2003. A Study on the Morphology , Karyology and
1078 Distribution of *Ellobius* Fischer , 1814 (Mammalia : Rodentia) in Iran.
1079 Turkish Journal of Zoology 27, 281–292.
- 1080 Neumann, K., Yiğit, N., Fritzsche, P., Çolak, E., Feoktistova, N., Surov, A.,
1081 Michaux, J., 2017. Genetic structure of the Turkish hamster (*Mesocricetus*
1082 *brandti*). Mammalian Biology 86, 84–91.
1083 <https://doi.org/10.1016/j.mambio.2017.06.004>
- 1084 Nishiaki, Y., Akazawa, T., 2018. The Middle and Upper Paleolithic Archeology
1085 of the Levant and Beyond. Replacement of Neanderthals by Modern
1086 Humans Series 35–47. https://doi.org/10.1007/978-981-10-6826-3_3
- 1087 Nowak, R.M., 1999. Walker's Mammals of the World. 6th ed. Baltimore, MD,
1088 USA: The Johns Hopkins University Press.
- 1089 Obuch, J., Khaleghizadeh, A., 2012. Spatial Variation in the Diet of the Barn
1090 Owl *Tyto alba* in Iran 6, 103–116.
- 1091 Osborn, D.J., 1962. Rodents of subfamily Microtinae from Turkey. J. Mammalia,
1092 43: 515-529.
- 1093 Rey-Rodríguez, I., Stoetzel, E., López-García, J.M., Denys, C., 2019.
1094 Implications of modern Barn owls pellets analysis for archaeological studies
1095 in the Middle East. Journal of Archaeological Science 111, 105029.
1096 <https://doi.org/10.1016/J.JAS.2019.105029>
- 1097 Roberts, T.J., 1977. The Mammals of Pakistan. London, UK: Ernst Benn Ltd.
1098

- 1099 Rusin, M., 2017. *Ellobius talpinus* , Northern Mole Vole. The IUCN Red List of
1100 Threatened Species 2016: e.T7656A115085720. 8235.
1101 [https://doi.org/http://dx.doi.org/10.2305/IUCN.UK.2016-](https://doi.org/http://dx.doi.org/10.2305/IUCN.UK.2016-3.RLTS.T7656A22339917.en)
1102 3.RLTS.T7656A22339917.en
- 1103 Sándor, A.D., 2018. Rediscovered after half a century: A new record of the grey
1104 dwarf hamster, *Cricetulus migratorius* (Mammalia: Cricetidae), in Romania.
1105 Turkish Journal of Zoology 42, 495–498. [https://doi.org/10.3906/zoo-1712-](https://doi.org/10.3906/zoo-1712-15)
1106 15
- 1107 Shehab, A., Daoud, A., Kock, D., Amr, Z., 2013. Zoology in the Middle East
1108 Small mammals recovered from owl pellets from Syria (Mammalia:
1109 Chiroptera,Rodentia). <https://doi.org/10.1080/09397140.2004.10638061>
- 1110 Shenbrot, G., Kryštufek, B., Molur, S., 2016. *Ellobius fuscocapillus* , Southern
1111 Mole Vole. The IUCN Red List of Threatened Species 2016:
1112 e.T7654A22339730. 8235.
1113 [https://doi.org/http://dx.doi.org/10.2305/IUCN.UK.2016-](https://doi.org/http://dx.doi.org/10.2305/IUCN.UK.2016-2.RLTS.T7654A22339730.en)
1114 2.RLTS.T7654A22339730.en
- 1115 Shenbrot, G., 2009. On the conspecificity of *Allactaga hotsoni* Thomas, 1920 and
1116 *Allactaga firouzi* Womochel, 1978 (Rodentia: Dipodoidea). Mammalia 73,
1117 231–237. <https://doi.org/10.1515/MAMM.2009.043>
- 1118 Shenbrot, G.I. and Krasnov, B.R. 2005. An Atlas of the Geographic Distribution
1119 of the Arvicoline Rodents of the World (Rodentia, Muridae: Arvicolinae).
1120 Pensoft Publishers, Sofia.
- 1121 Siahsarvie, R., Darvish, J., 2008. Geometric morphometric analysis of Iranian
1122 wood mice of the genus *Apodemus* (Rodentia, Muridae). Mammalia 72,
1123 109–115. <https://doi.org/10.1515/MAMM.2008.020>
- 1124 Smith, K.T., Christian, L., Flemming, F., Barkai, R., Gopher, A., 2016. The
1125 microvertebrates of Qesem Cave : A comparison of the two concentrations.
1126 Quaternary International 1–13. <https://doi.org/10.1016/j.quaint.2015.04.047>
- 1127 Souttou, K., Denys, C., 2012. Small Mammal Bone Modifications in Black-
1128 Shouldered Kite *Elanus caeruleus* Pellets from Algeria : Implications for
1129 Archaeological Sites. Journal of Taphonomy 10, 1–19.

- 1130 Stoetzel, E., Cornette, R., Lalis, A., Nicolas, V., Cucchi, T., Denys, C., 2017.
1131 Systematics and evolution of the *Meriones shawii/grandis* complex
1132 (Rodentia, Gerbillinae) during the Late Quaternary in northwestern Africa:
1133 Exploring the role of environmental and anthropogenic changes.
1134 Quaternary Science Reviews 164, 199–216.
1135 <https://doi.org/10.1016/j.quascirev.2017.04.002>
- 1136 Tesakov, A.S., 2016. Early Middle Pleistocene *Ellobius* (Rodentia , Cricetidae ,
1137 Arvicolinae) from Armenia. Russian J. Theriol. 15 (2): 151–158.
- 1138 Thomas, O., 1905. *Ellobius woosnami*. Abstr. Proc. Zool. Soc. 23; Proc. Zool.
1139 Soc. 526 London.
- 1140 Tsytulina, K., Kryštufek, B., Yigit, N., Bukhnikashvili, A., Shenbrot, G., 2017.
1141 *Microtus socialis* , Social. The IUCN Red List of Threatened Species 2016:
1142 e.T13458A115114745.
1143 8235.[https://doi.org/http://dx.doi.org/10.2305/IUCN.UK.2016-](https://doi.org/http://dx.doi.org/10.2305/IUCN.UK.2016-3.RLTS.T13458A22348936.en)
1144 [3.RLTS.T13458A22348936.en](https://doi.org/http://dx.doi.org/10.2305/IUCN.UK.2016-3.RLTS.T13458A22348936.en)
- 1145 Walker, E.P., 1964. Mammals of the World. Vol. 2. Baltimore, MD,USA: The
1146 Johns Hopkins Press.
- 1147 Weissbrod, L., Zaidner, Y., 2014. Taphonomy and paleoecological implications
1148 of fossorial microvertebrates at the Middle Paleolithic open-air site of
1149 Neshet Ramla, Israel. Quaternary International 331, 115–127.
1150 <https://doi.org/10.1016/j.quaint.2013.05.044>
- 1151 Wilson, D.E. and Reeder, D.M., 2005. Mammal Species of the World.
1152 Washington, DC, USA: Smithsonian Institution Scholarly Press.
- 1153
- 1154